Supplementary Information for:

High Yielding Synthesis of Chiral Donor-Acceptor Catenanes

Mehrafarin Eilbigi Dehkordi,[a] Vijay Luxami [ab] and G. Dan Pantoș*[a]

a) *University of Bath, Department of Chemistry, Calverton Down, Bath, BA27AY, UK.*
b) *Current Address:School of Chemistry and Biochemistry, Thapar University, Patiala, INDIA 147004*

Table of Contents

1. Experimental

HPLC method for DCLs of $A1D_2$, $A1^*D_2$ and $A2^*D_2$ (5 mM):

Column: Develosil RPAqueous-3 C_{30}, 5.0 x 0.3 cm, 3 μm

Injection volume	3 μL
Flow Rate	0.5 mL/min
Temperature	38 °C
Run Time	25 min
Elution Profile	Gradient elution by CH_3CN/Water (0.1% FA)

Time/ min	**Water (0.1% FA)**	**CH_3CN (0.1% FA)**
0	85%	15%
25	40%	60%
30	85%	15%

Preparative method for DCLs of $A1D_2$ and $A1^*D_2$ (5 mM):

Column: Develosil 5u Combi-RP C_{30}, 5.0 x 2.0 cm, 5 μm

Injection volume	300 μL
Flow Rate	4 mL/min
Temperature	38 °C
Run Time	30 min
Elution Profile	Gradient elution by CH_3CN/Water (0.1% FA)

Time/ min	**Water (0.1% FA)**	**CH_3CN (0.1% FA)**
0	80%	20%
30	55%	45%
40	80%	20%

Analytical method for DCL of $A2D_2$ (5 mM):

Column: Kromasil C_8 5u, 25.0 x 0.46 cm, 5 μm.

Injection volume	3 μL
Flow Rate	0.5 mL/min
Temperature	38 °C
Run Time	25 min
Elution Profile	Gradient elution by CH_3CN/Water (0.1% FA)

Time/ min	**Water (0.1% FA)**	**CH_3CN (0.1% FA)**
0	80%	20%
25	35%	65%
30	80%	20%

Preparative method for DCLs of $A2D_2$ and $A2^*D_2$ (5 mM):

Column: Kromasil 100-5 C_8, 25.0 x 0.8 cm, 5 μm

Injection volume	400 μL
Flow Rate	3 mL/min
Temperature	38 °C
Run Time	30 min
Elution Profile	Gradient elution by CH_3CN/Water (0.1% FA)

Time/ min	**Water (0.1% FA)**	**CH_3CN (0.1% FA)**
0	75%	25%
30	55%	45%
40	75%	25%

2. Analysis of the species present in the library *via* HPLC

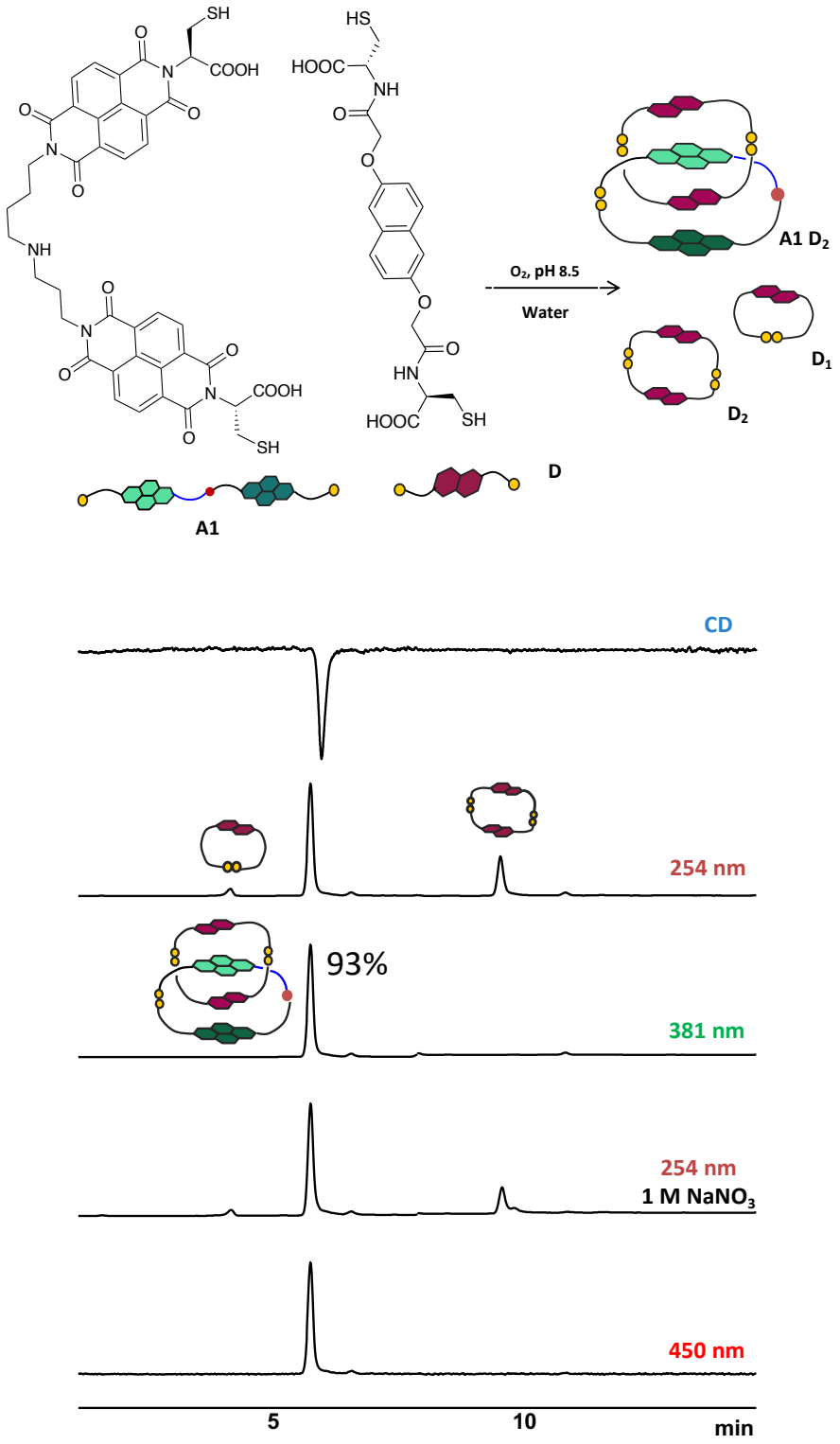

Figure S1. The HPLC analysis of **A1** and **D** DCL (1:2 molar ratio, 5mM total concentration, H_2O).

LC-MS Analysis

MS spectra of the species identified in the aqueous library of **A1** with **D**.

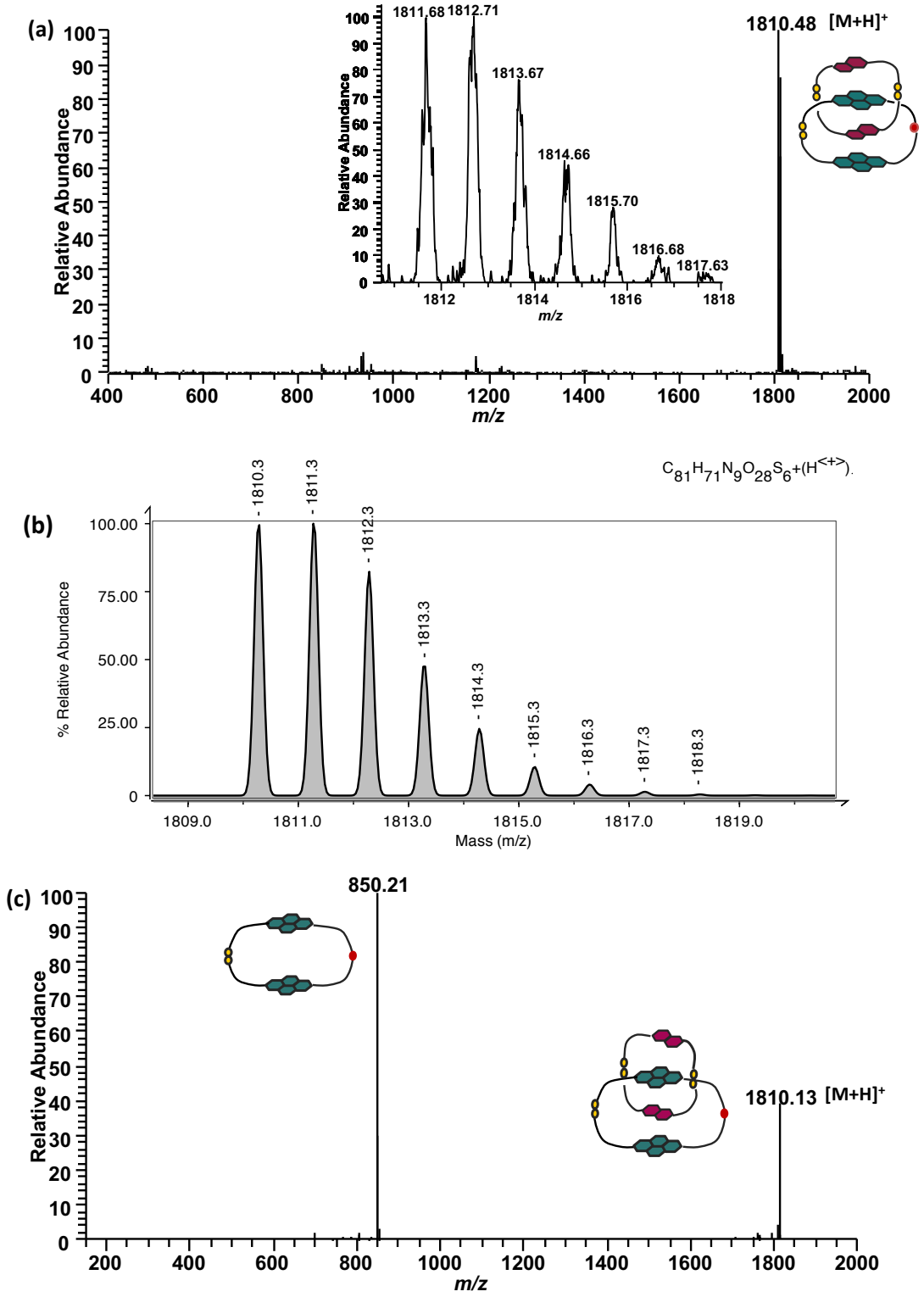

Figure S2. (a) Full MS (*+ve*), (b) Theoretical MS spectrum (*+ve*) and (c) MS/MS fragmentation of **A1D$_2$**.

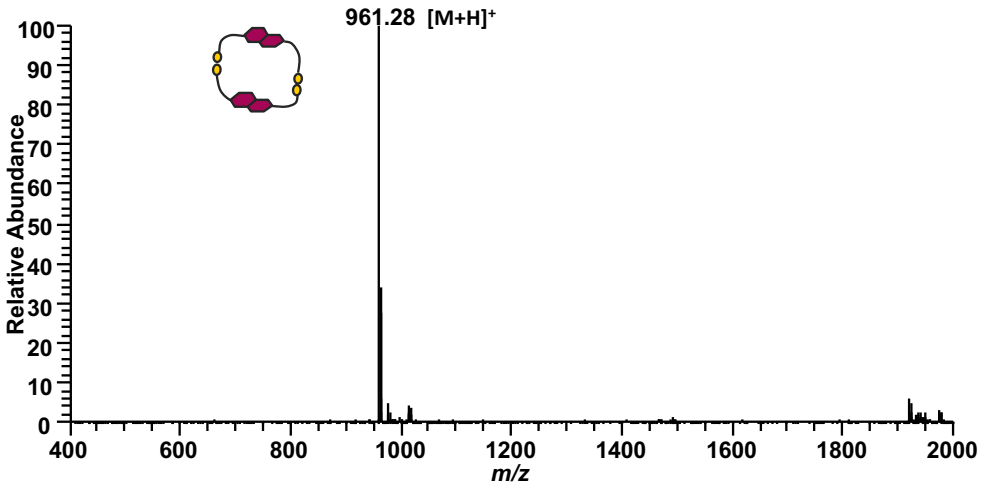

Figure S3. The experimental ESI-MS spectrum (*+ve*) of **D_2**.

The ESI-MS and MS/MS fragmentation patterns are in agreement with the proposed structure of **$A1D_2$** and **D_2**.

3. 1D and 2D ^{1}H NMR Characterisation of $A1D_2$

In order to confirm that the peak at 5 min is a catenane and not a macrocycle, it was isolated by preparative HPLC (isolated yield: 97% pure, Figure S4) and analysed by NMR and CD.

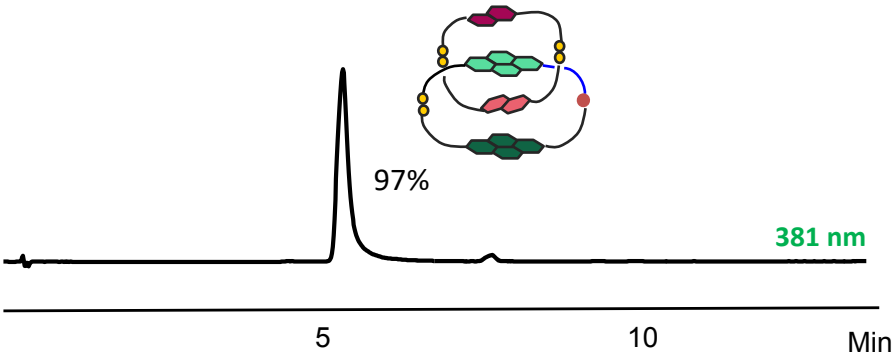

Figure S4. Reverse-Phase HPLC result of the isolated catenane. Absorbance was recorded at 381 nm.

The NMR analysis shows very sharp NMR signals in D_2O (500 MHz) and this is an indication of rigidity through complex topology of the structure, whereas macrocycles usually give very broad NMR signals due to their flexibility.

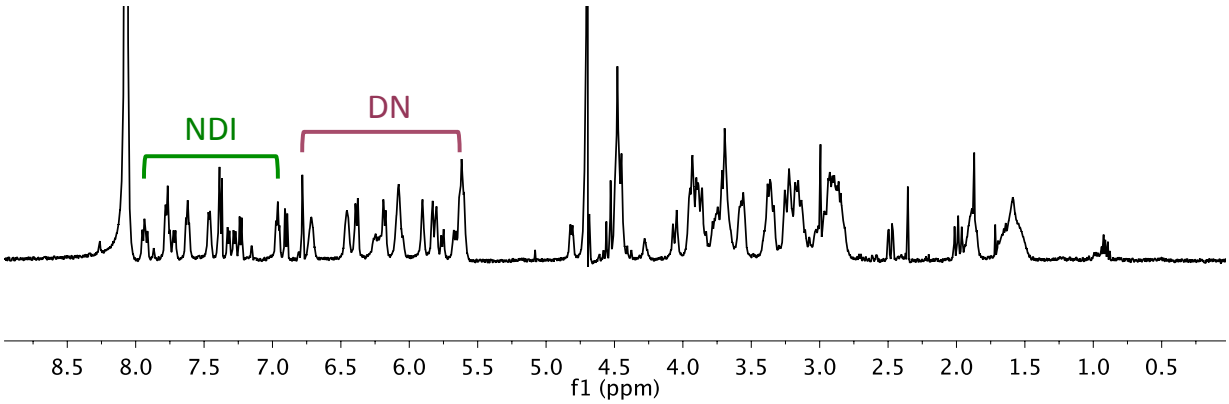

Figure S5. ^{1}H NMR full spectrum of the **A1D$_2$** catenane in D_2O (500 MHz). The solvent peak was referenced at 4.74 ppm).

Due to the lack of symmetry in the structure of **A1D$_2$** catenane, it is produced as a pair of diastereomers, each having two conformers.

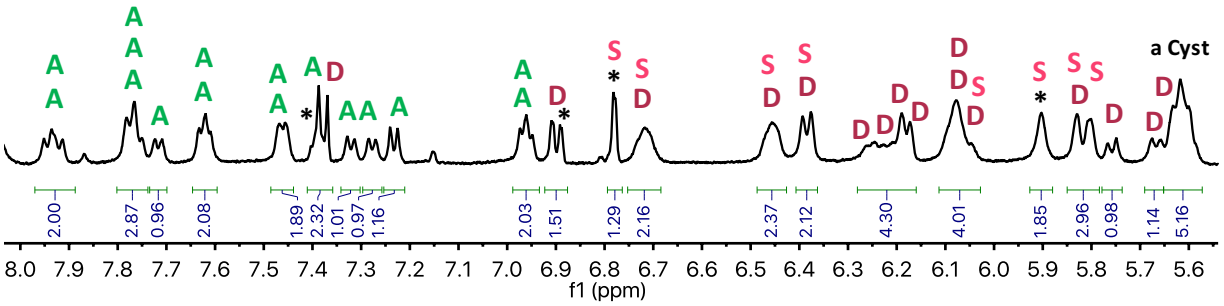

Figure S6. Partial ^{1}H NMR spectrum of **A1D$_2$** catenane across 5.4 – 8.0 ppm region in D_2O. The **A** = signals corresponding to the NDI core, **D** = signals corresponding to the two doublets on the dialkoxynphthalene, and **S =** represents the singlet peak of the dialkoxynphthalene; the ***** represents impurity.

The ^{1}H NMR of **A1D$_2$** is consequently extremely complex, however, analysis of the donor and acceptor regions by employing the COSY and NOESY spectra allowed correlation of the signals expected from a mixture of four isomeric catenanes.

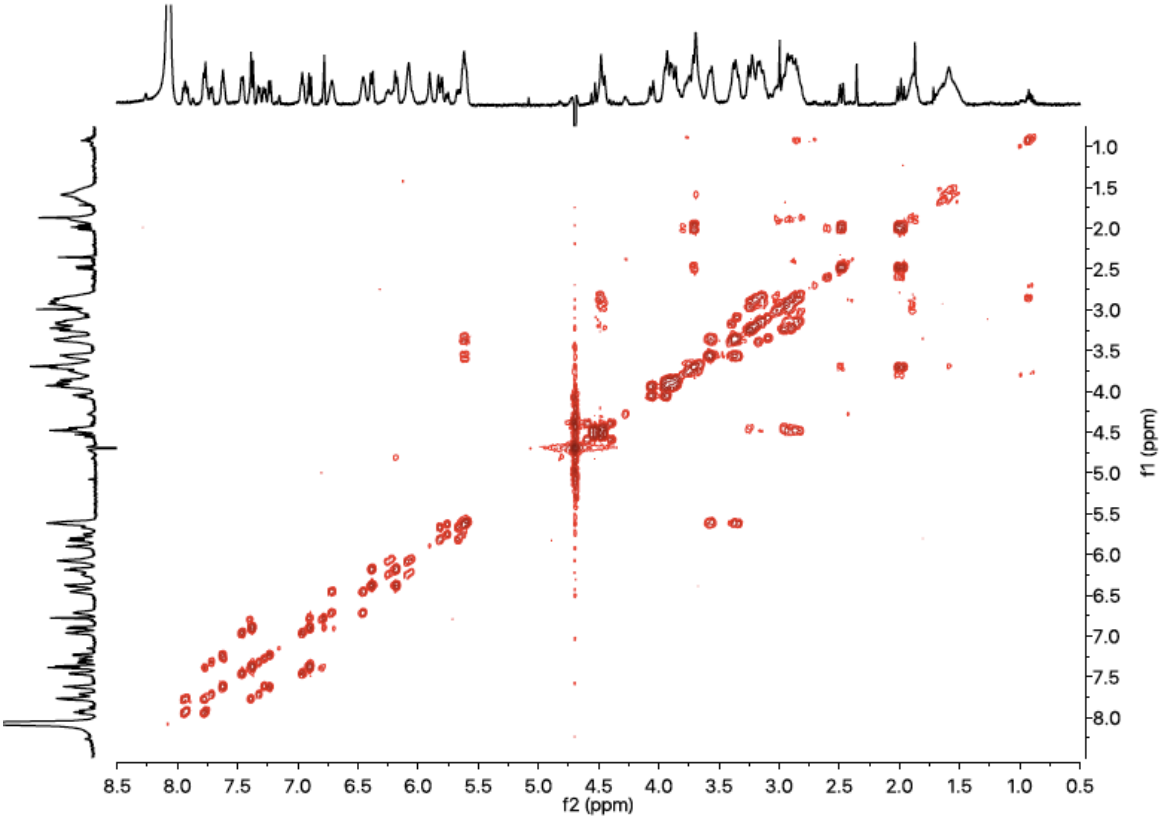

Figure S7. Full COSY spectrum of **A1D$_2$** (D_2O, 500 MHz, the solvent peak was referenced at 4.74 ppm).

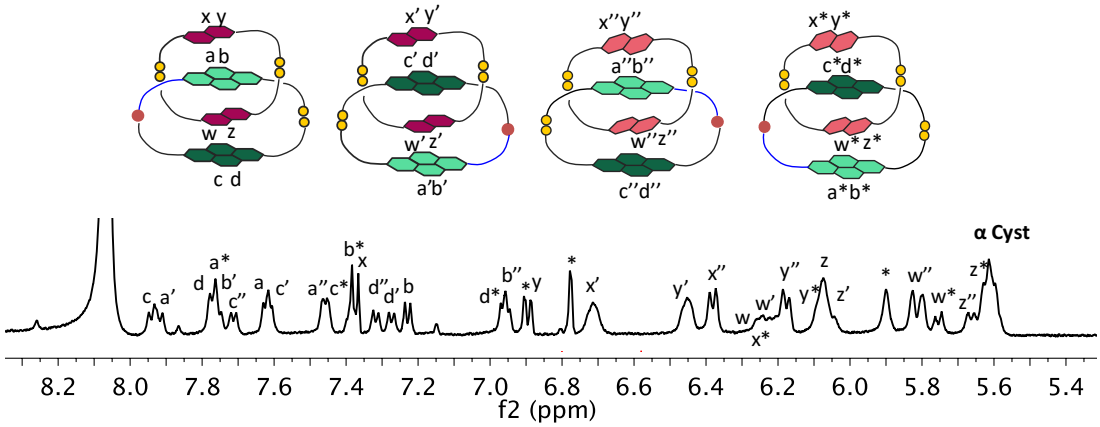

Figure S8. Partial COSY spectrum of **A1D$_2$** catenane between 5.4 – 8.2 ppm region (D_2O, 500 MHz).

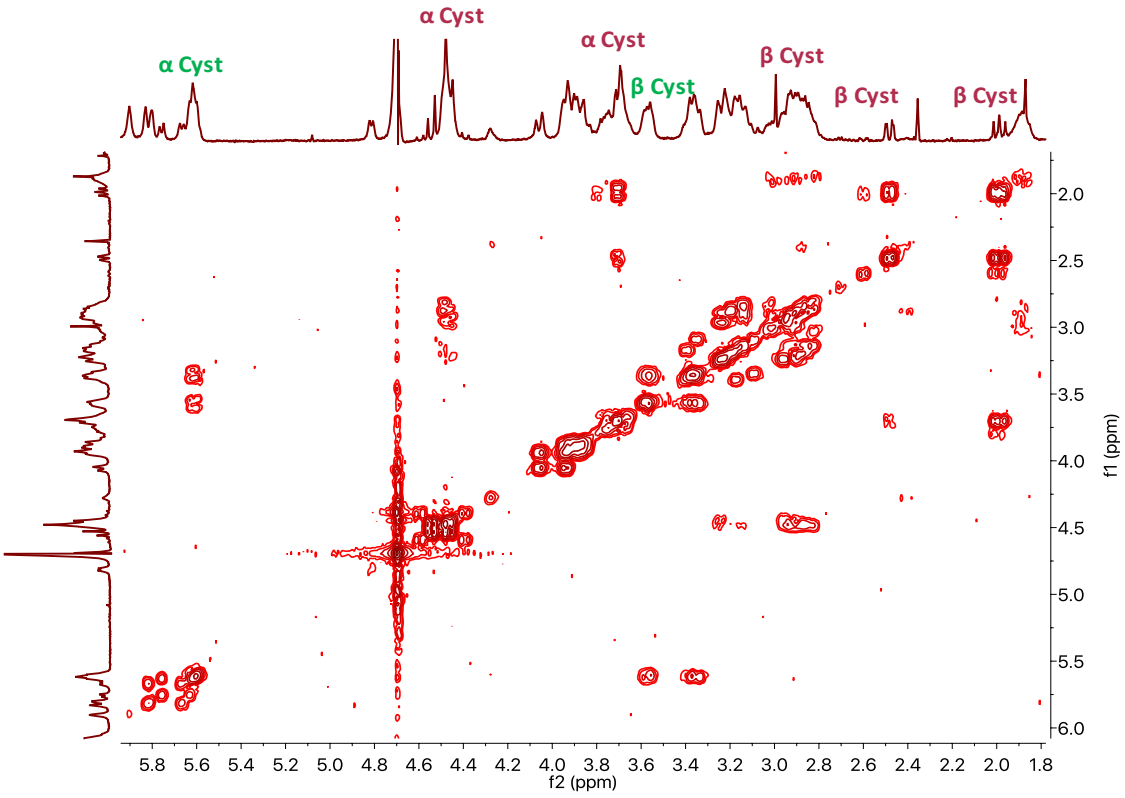

Figure S9. Partial COSY spectrum of **A1D$_2$** catenane between 1.8 – 5.6 ppm region (D_2O, 500 MHz).

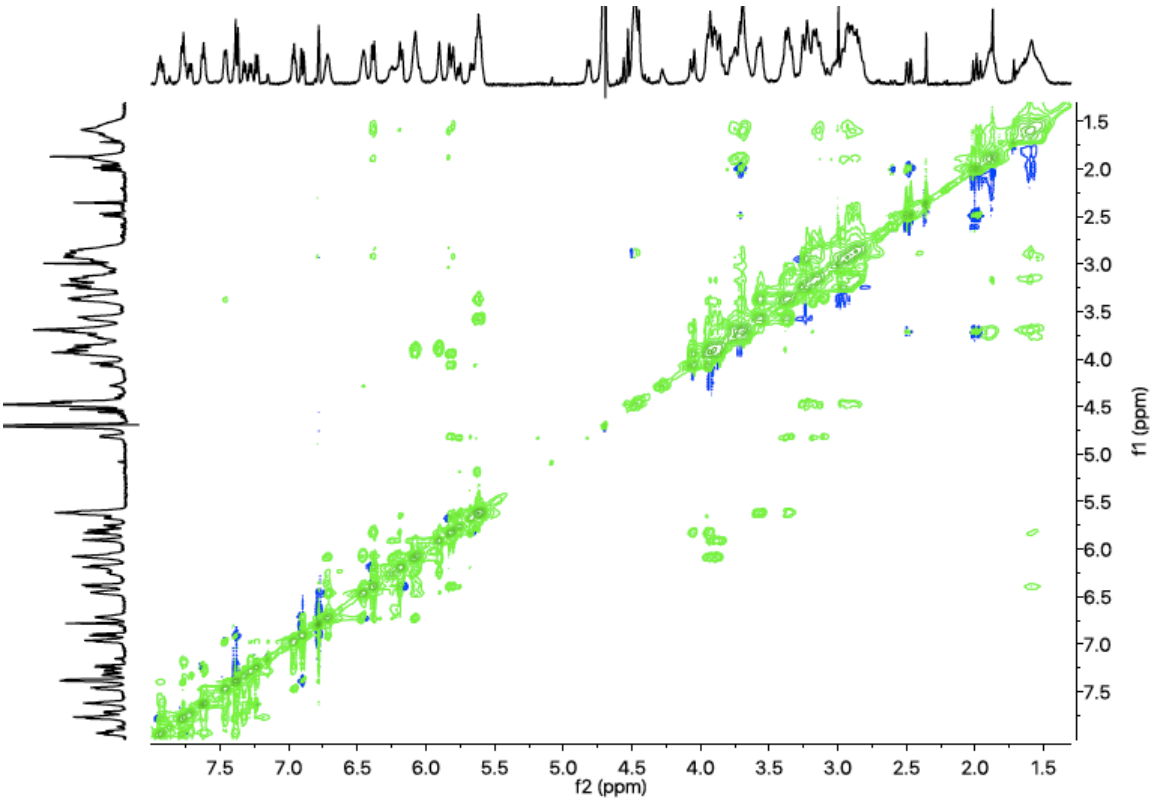

Figure S10. Full NOESY spectrum of **A1D$_2$** catenane (D2O, 500 MHz).

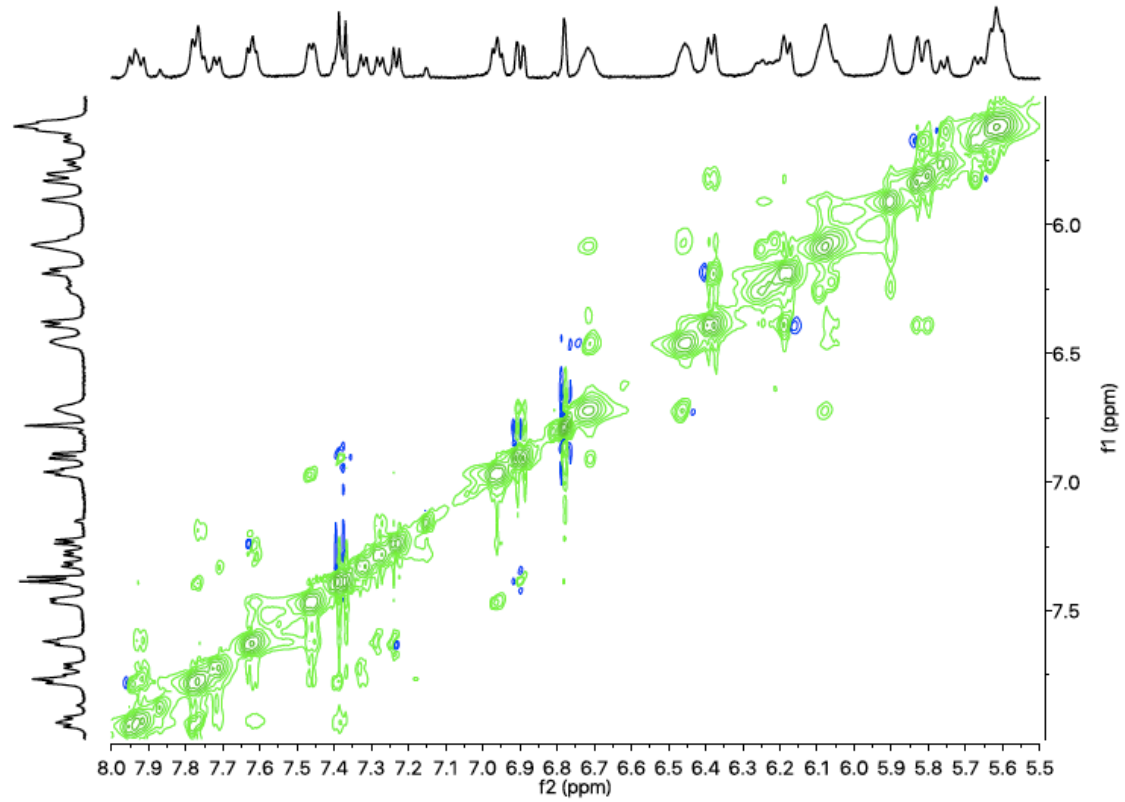

Figure S11. Partial NOESY spectrum of **A1D$_2$** catenane across 5.5 – 8.0 ppm region (D_2O, 500 MHz).

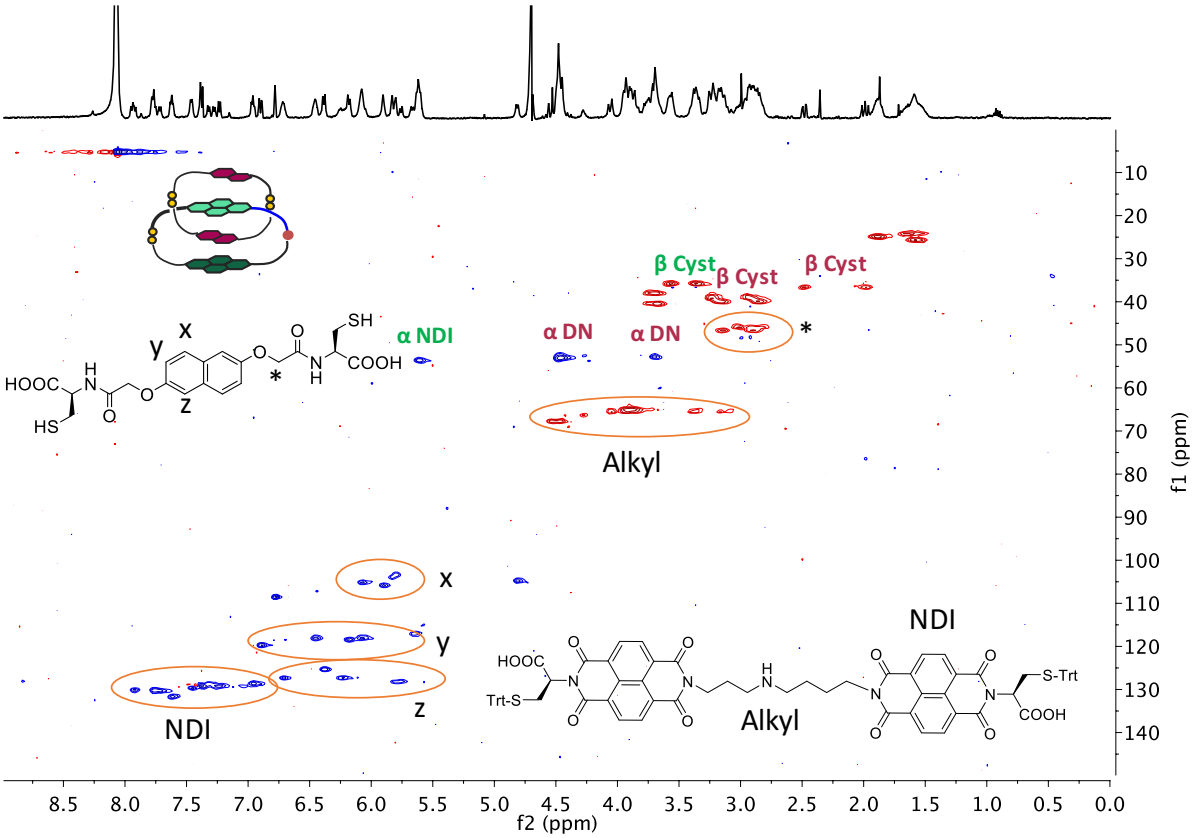

Figure S12. Full HSQC spectrum of **A1D$_2$** catenane (D2O, 500 MHz).

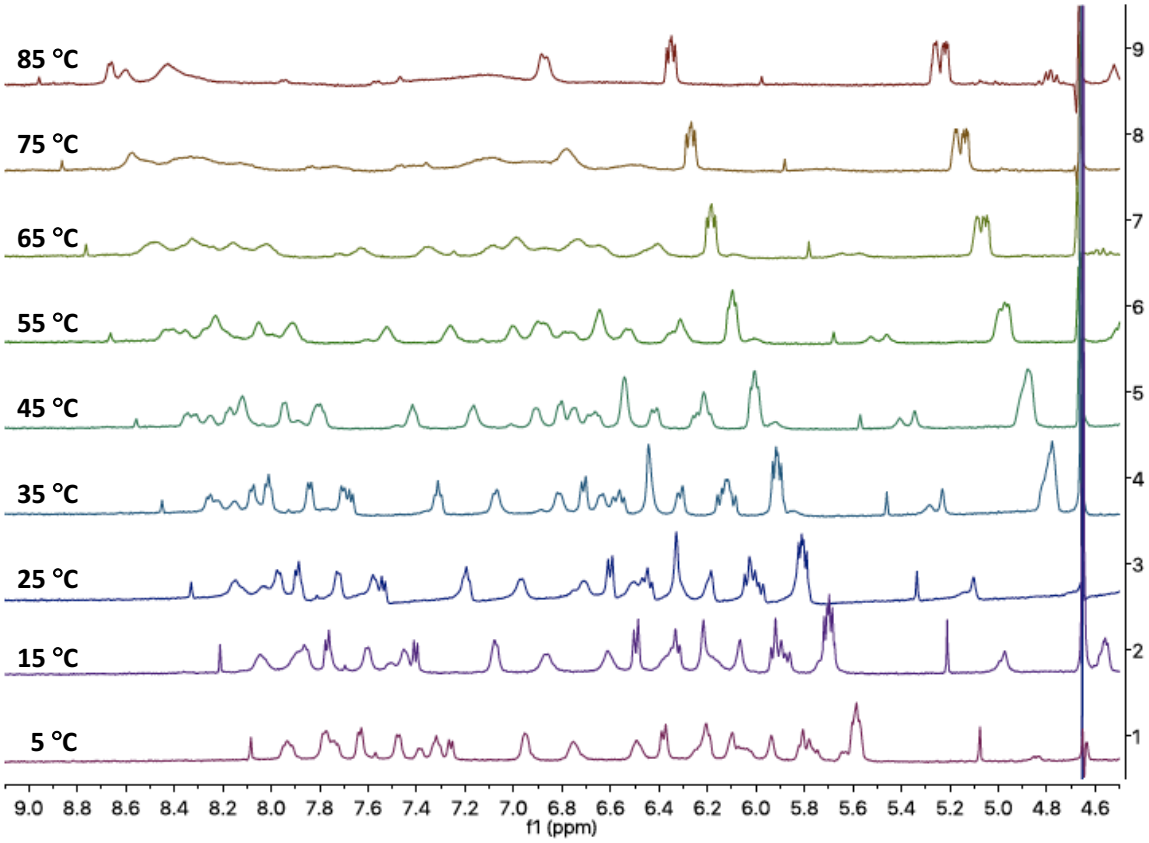

Figure S13. ^{1}H NMR spectrum of **A1D$_2$** at various temperatures (D_2O, 500 MHz).

4. Circular Dichroism (CD) Analysis of A1D$_2$

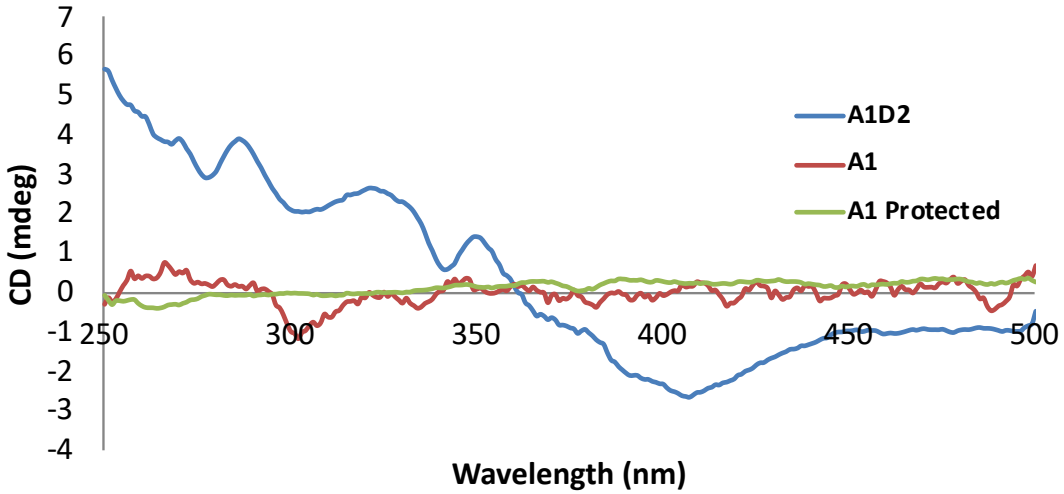

Figure S14. The CD signal of the **A1D$_2$** catenane is compared to the **A1** protected and deprotected on the thiol. These spectra highlight that the induced CD signal around 400 nm in the catenane is orders of magnitude stronger than in related interlocked structures. (**A1D$_2$** and **A1** in D_2O, **A1** protected in CH_3CN, 250 – 550 nm, 10 mm cuvette pathlength).

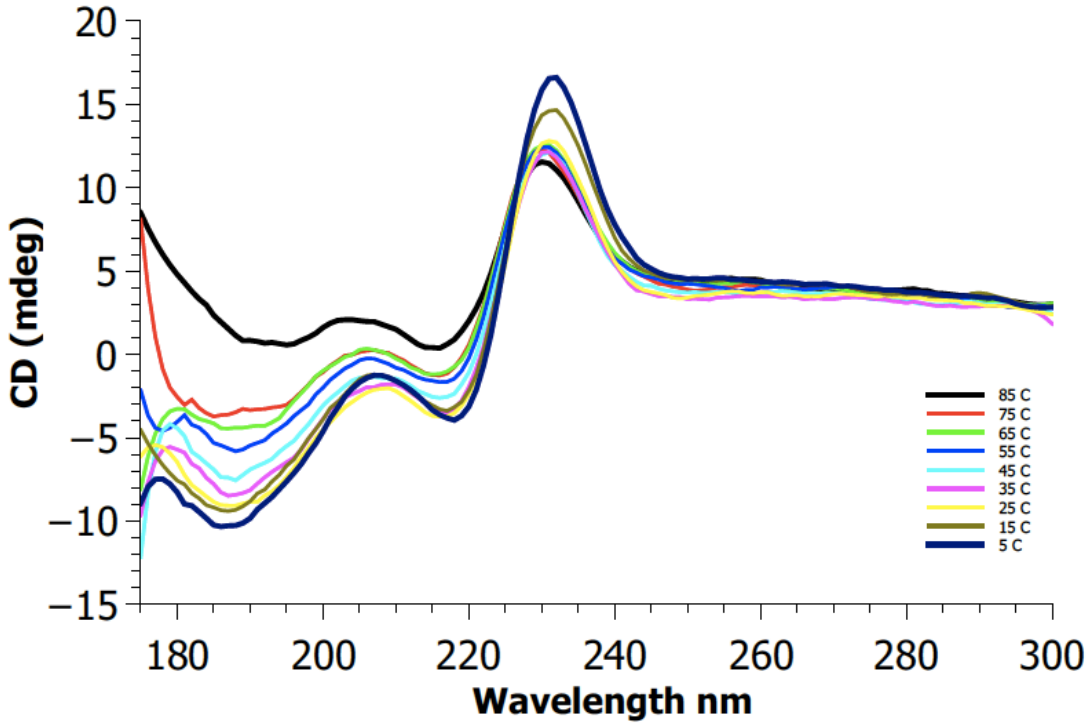

Figure S15. Variable temperature CD spectra between 5 – 85 °C of **A1D$_2$** (D_2O, 175 – 300 nm, 1 mm cuvette pathlength).

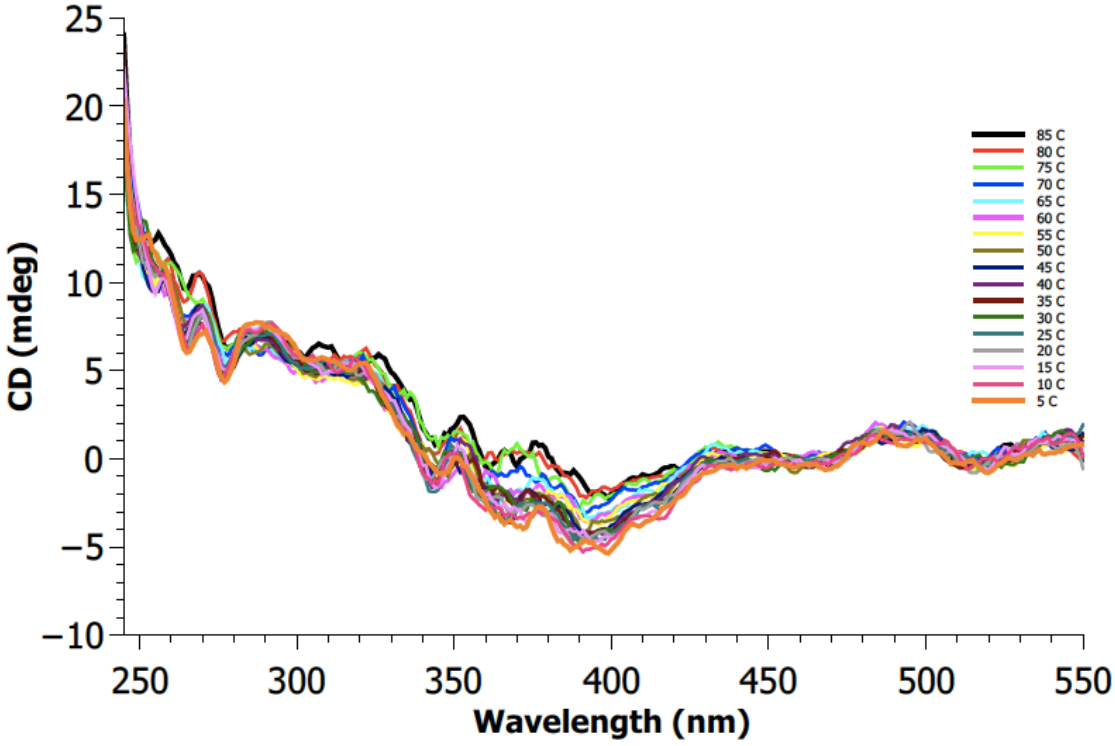

Figure S16. Variable temperature CD spectra between 5 – 85 °C of **A1D$_2$** (D_2O, 245 – 550 nm, 10 mm cuvette pathlength).

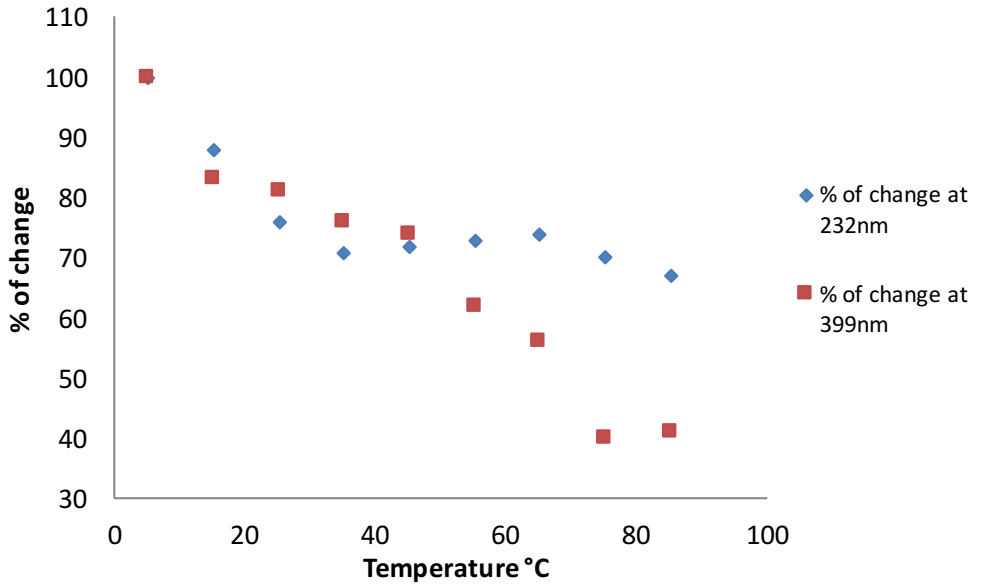

Figure S17. The comparison between % of change at two wavelengths (232 and 399 nm) of **A1D$_2$**. The % of change illustrates the variation of CD intensity at different temperatures. This study shows that there is more flexibility at the higher wavelength (which is the NDI region of catenane) than the cysteine region.

5. DCL Library in Large Volume

The library of **A1** and **D** was also made in large volume to compare the libraries distribution with the 1 mL libraries. The slight erosion in yield is due to an error in relative ratio of the building blocks due to the hygroscopicity of the TFA salt of the **A1** building block.

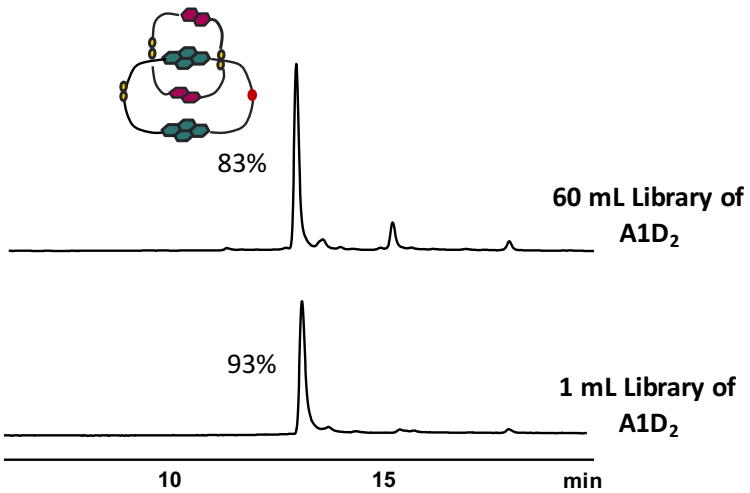

Figure S18. The HPLC analysis of **A1** and **D** (1:2 molar ratio, 5 mM total concentration, H_2O). Absorbance was recorded at 381 nm.

6. The Effect of Chirality on Catenane Formation

Alteration of cysteine chirality from L to D on NDI molecule led to a library with a similar distribution, the only difference being a slight change in the retention time of **A1*D$_2$** to **A1D$_2$** catenane. This is expected since the two catenanes only differ in point chirality of two atoms, while having the same topology.

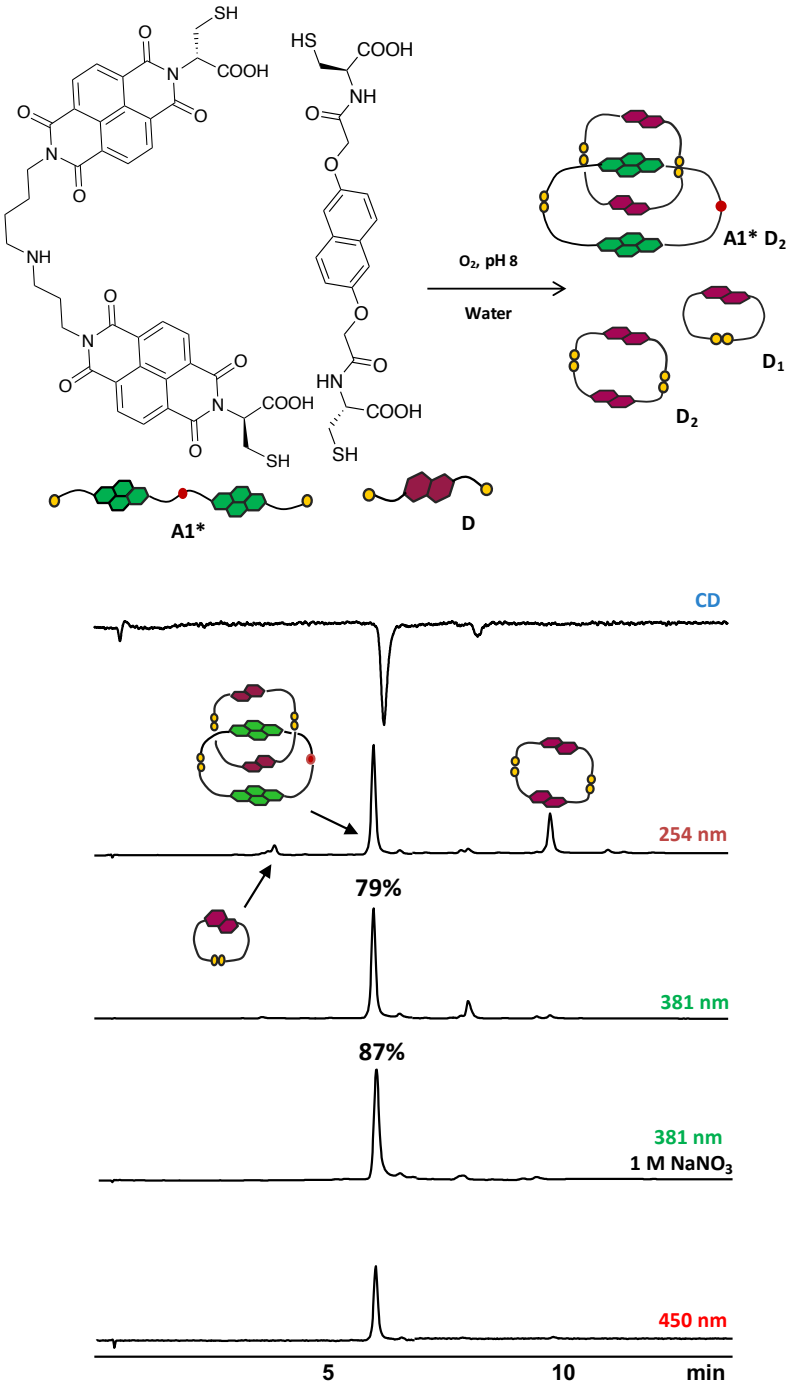

Figure S19. The HPLC analysis of **A1*** and **D** (1:2 molar ratio, 5 mM total concentration).

Kinetic Study of A1*D_2 Formation

The kinetic study for formation of **A1*D$_2$** was performed on the **A1*** and **D** library over time (1:2 molar ratio, Figure S20 and S21). The presence of intermediates and macrocyclic species at the start of library is expected, which ultimately fall into the thermodynamic sink that represents the formation of the [2]catenane.

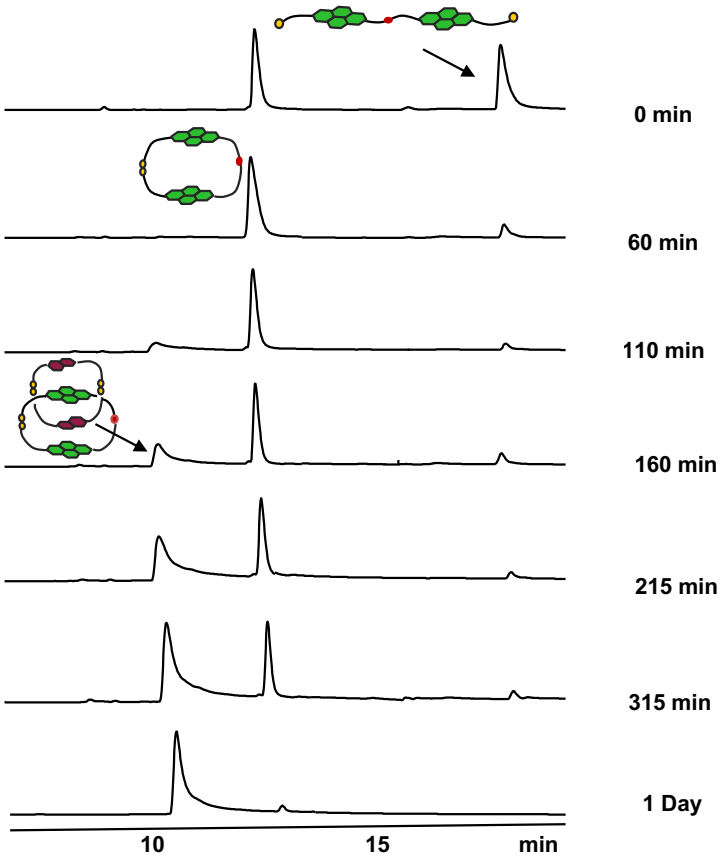

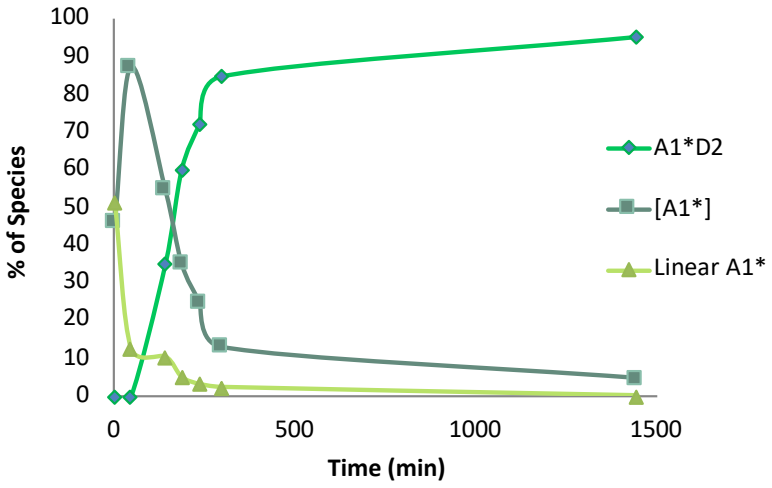

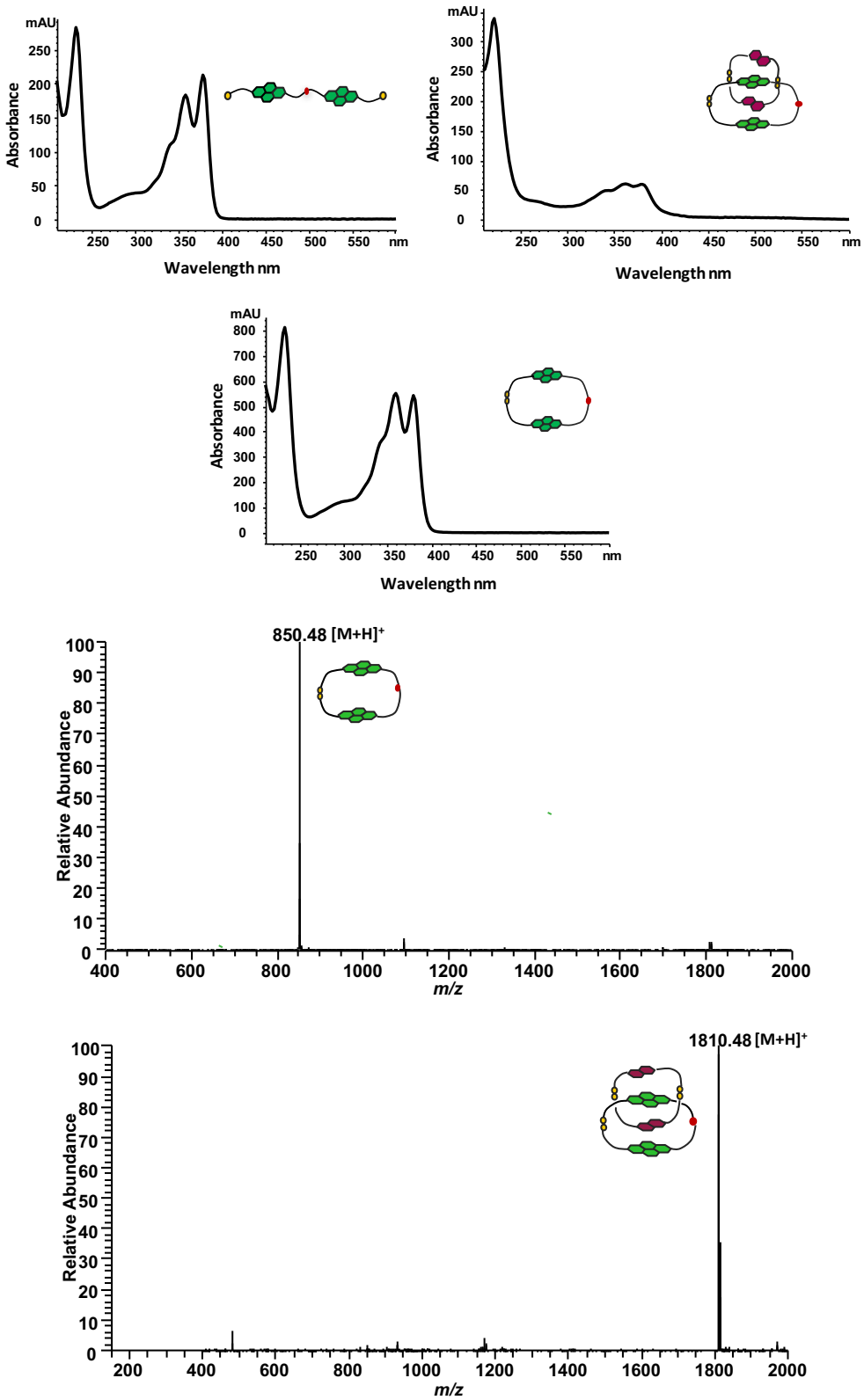

Figure S20. Kinetic study showing the formation of **A1*D$_2$** over time. Absorbance was monitored at 381 nm. The UV-Vis spectrum shows the UV of each peak corresponding to the correct structure and full ESI-MS (*+ve*) of cyclic **A1*** monomer and **A1*D$_2$** catenane also confirms the structures.

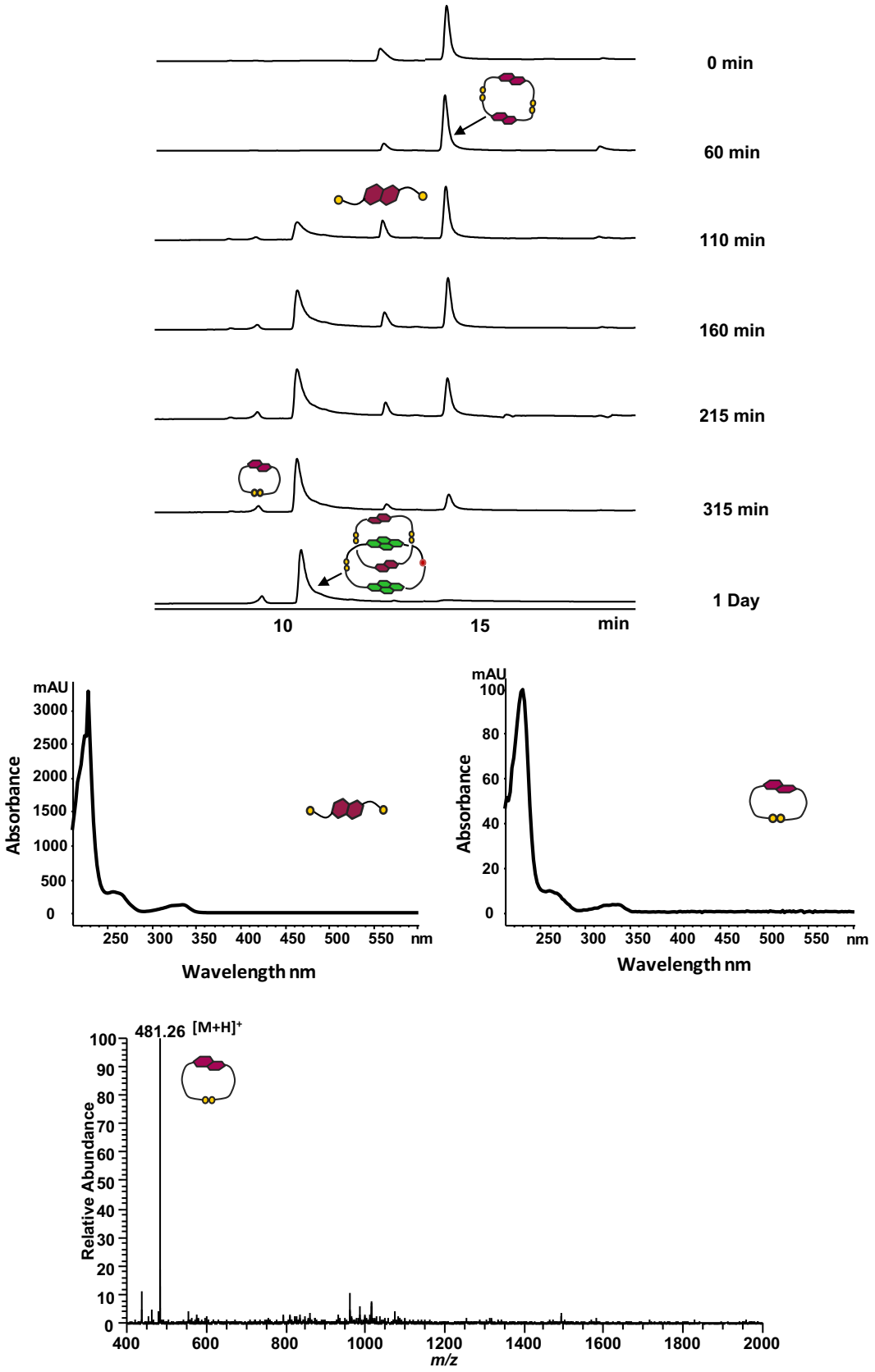

Figure S21. Kinetic study showing the formation of **A1*D$_2$** over time. Absorbance was monitored at 254 nm. The UV-Vis spectrum of **D** and **D$_2$** and full MS (*+ve*) of cyclic **D$_1$** corresponding to the correct structure.

7. Circular Dichroism (CD) Analysis of A1*D_2

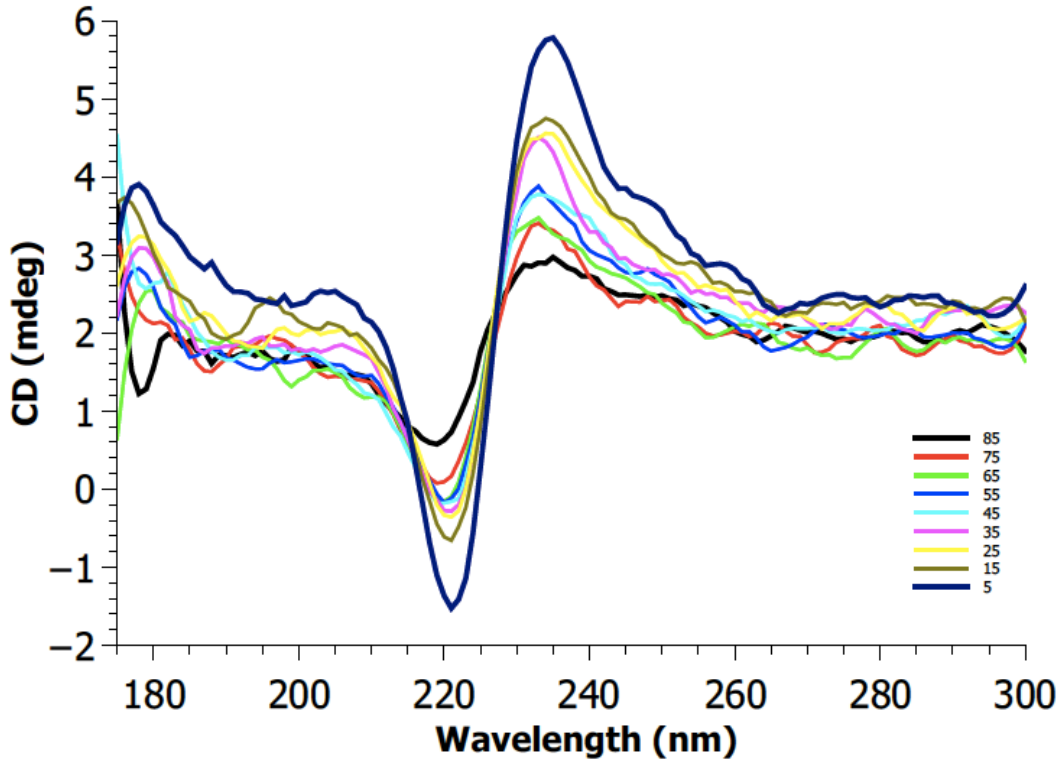

Figure S22. Variable temperature CD spectra between 5 – 85 °C of **A1*D_2** (D_2O, 175 – 300 nm, 1 mm cuvette pathlength).

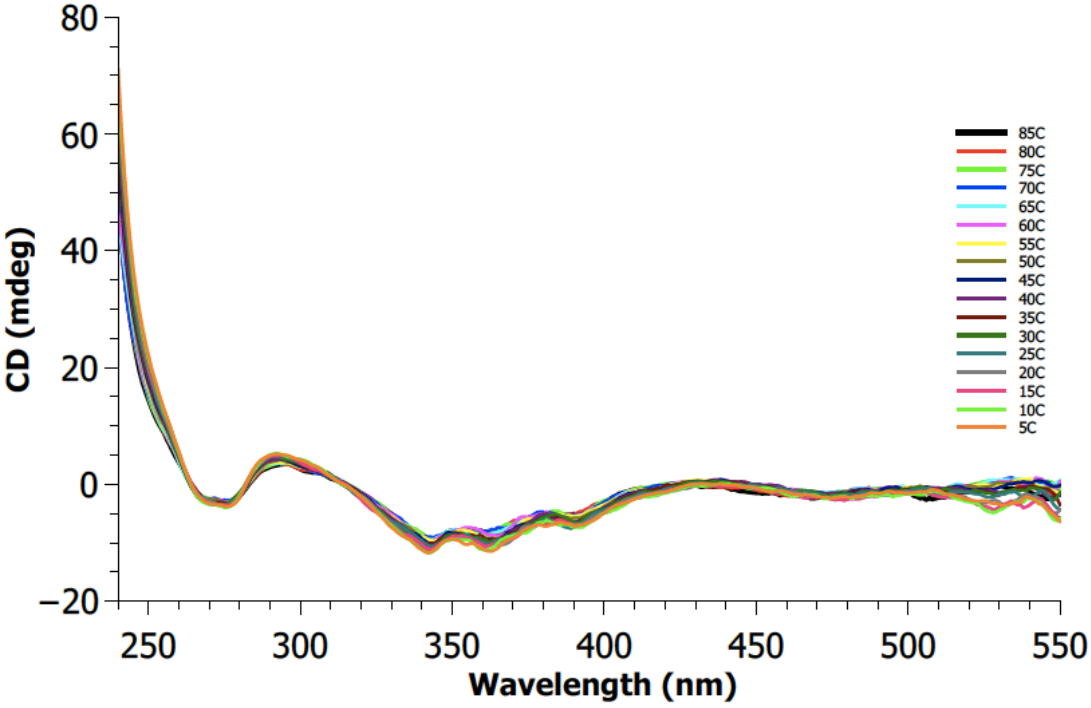

Figure S23. Variable temperature CD spectra between 5 – 85 °C of **A1*D_2** (D_2O, 245 – 550 nm, 10 mm cuvette pathlength).

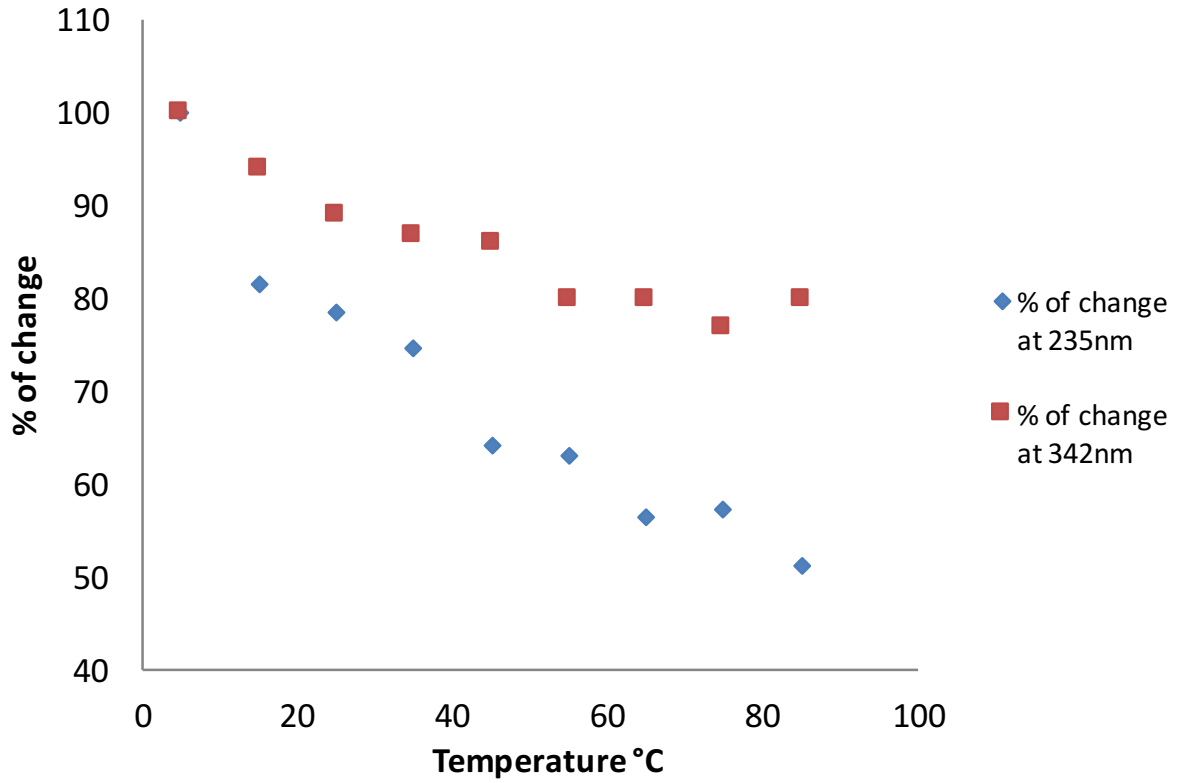

Figure S24. The comparison between % of change in two wavelengths (235 and 342 nm) of **A1*D$_2$**. This catenane, **A1*D$_2$**, unlike **A1D$_2$** displays more flexibility across the cysteine region, and therefore the % of change is greater at lower wavelength.

8. Synthesis of $A1D_2$ and $A1^*D_2$ catenanes in different conditions

The variation of (**A1** - **D**) and (**A1*** - **D**) building blocks ratio led to the formation of new molecules such as different macrocycles and their identification by HPLC analysis and MS spectra.

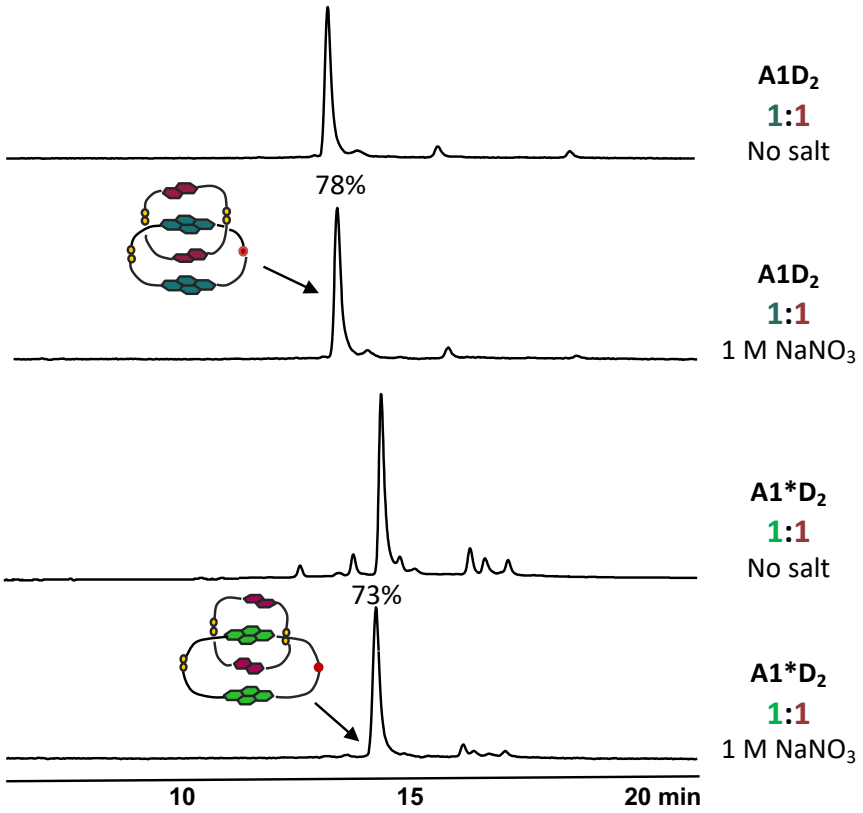

Figure S25. The **$A1D_2$** and **$A1^*D_2$** catenanes form up to 78 and 73% respectively in libraries with 1:1 ratio of the two building blocks (381 nm).

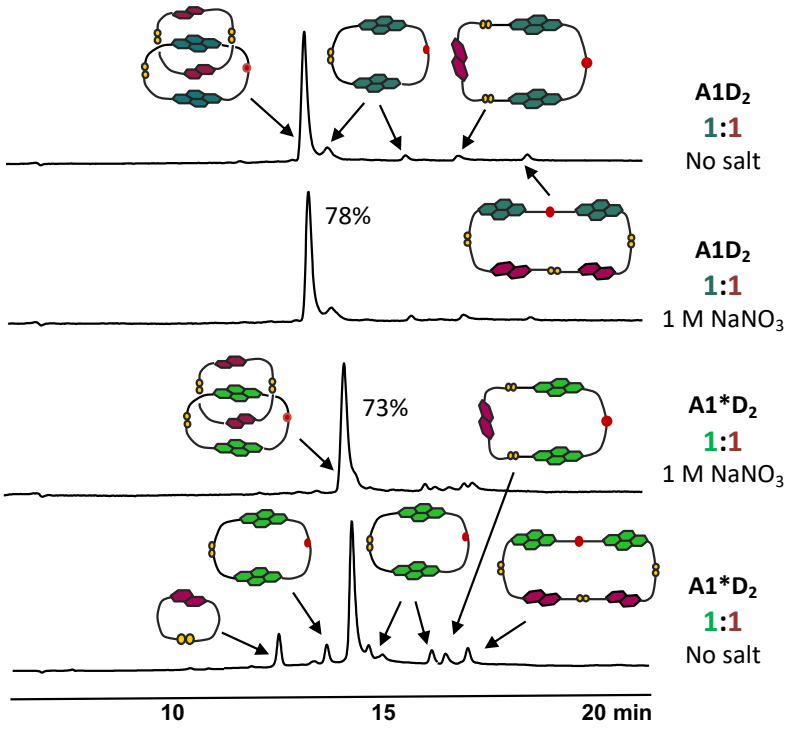

Figure S26. Identification of new macrocycles at 254 nm.

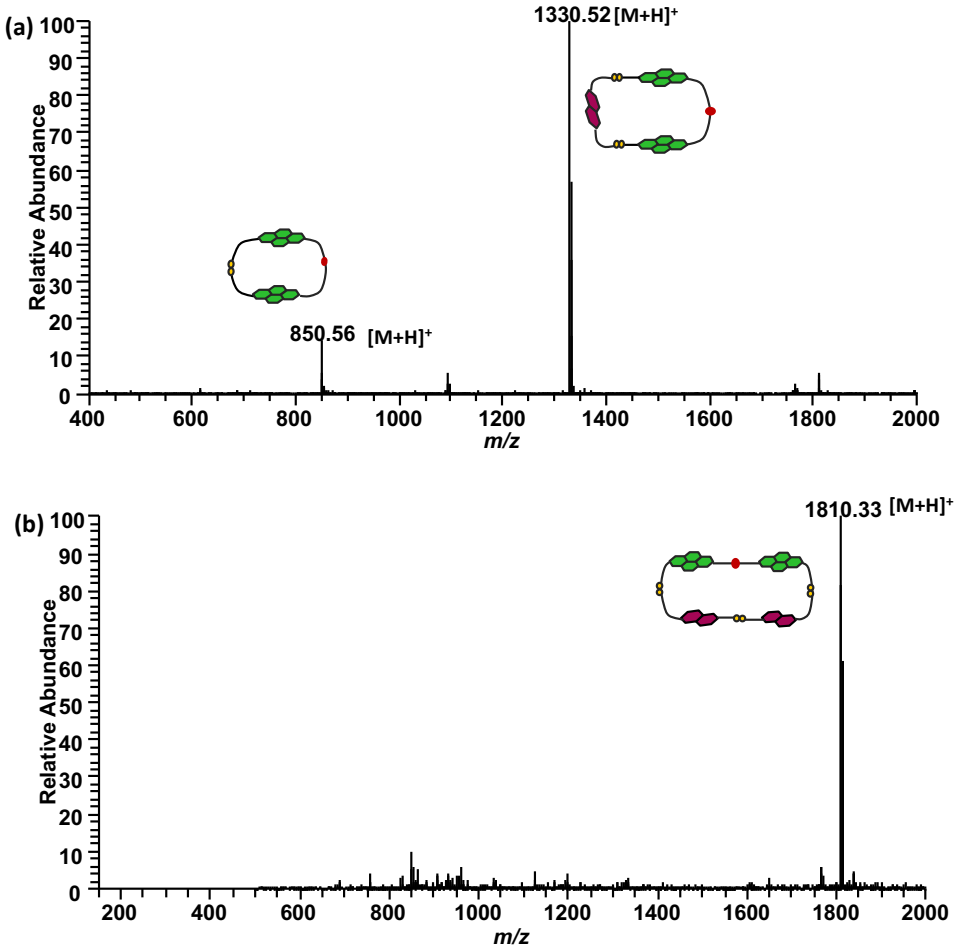

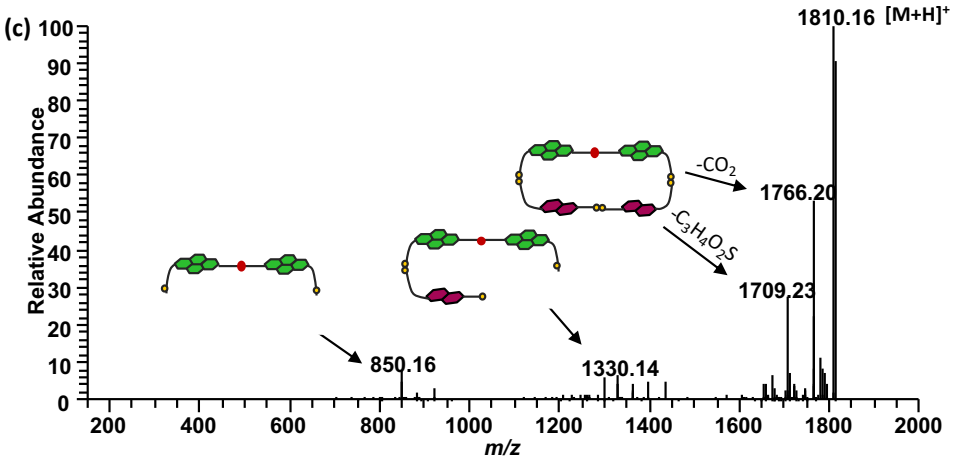

Figure S27. ESI-MS (+ve) spectra of the species identified in the aqueous library of **A1*** with **D** in 1:1 ratio: a) cyclic **A1*D**, b) **A1*D$_2$** macrocycle, and c) MS-MS fragmentation spectra of the **A1*D$_2$** macrocycle.

9. Effect of Tetrabutylamonium Nitrate on Formation of Catenane

It has been proven from previous studies that the addition of salts such as $NaNO_3$ can amplify the formation [2]catenanes by increasing the polarity of the solvent. However, addition of templates such as tetrabutylammonium nitrate, (Bu_4NNO_3), can actually have a negative effect on formation of the [2]catenanes because Bu_4N^+ can solvate the NDI surface and therefore lead to a different library distribution, amplifying the cyclic **D_2** and cyclic **A1*** at the expense of the [2]catenane.

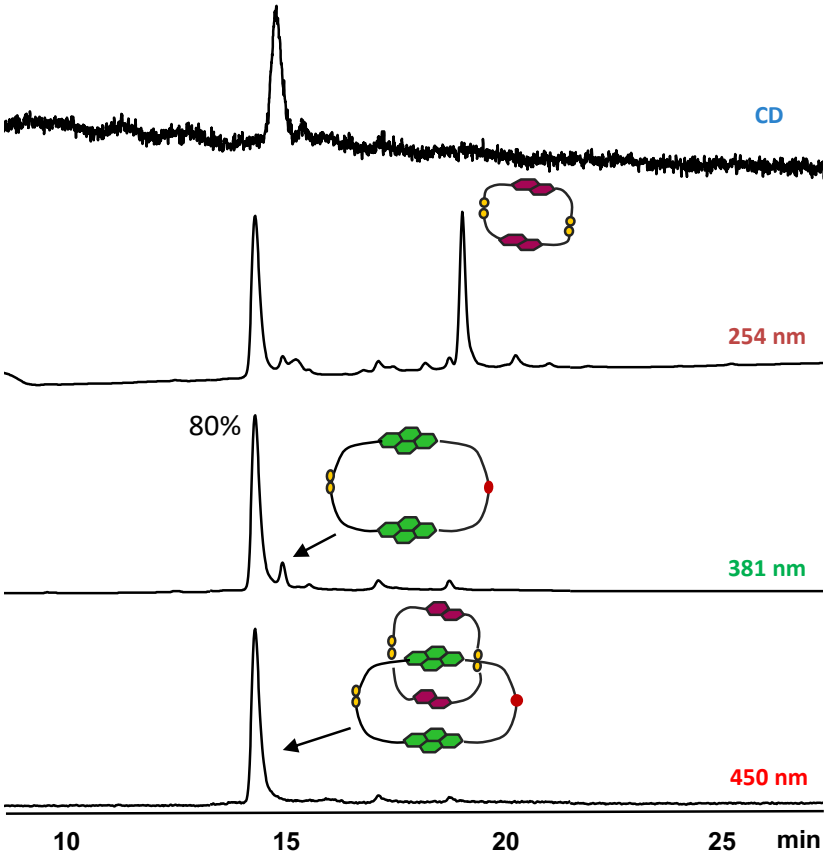

Figure S28. Effect of Bu_4NNO_3 salt on the library's distribution (5 mM, H_2O, 1 M salt, pH 8).

10. Effect of Polarity of solvent on Formation of Catenane

In order to provide a comprehensive study about the effect of solvent polarity on formation of these [2]catenanes (**A1D$_2$** and **A1*D$_2$**), the libraries were set-up in a lower polarity solvent (acetonitrile:water 1:1 ratio). The results from HPLC show that the addition of acetonitrile reduces both the polarity of solvent and the % yield of the **A1*D2** catenane.

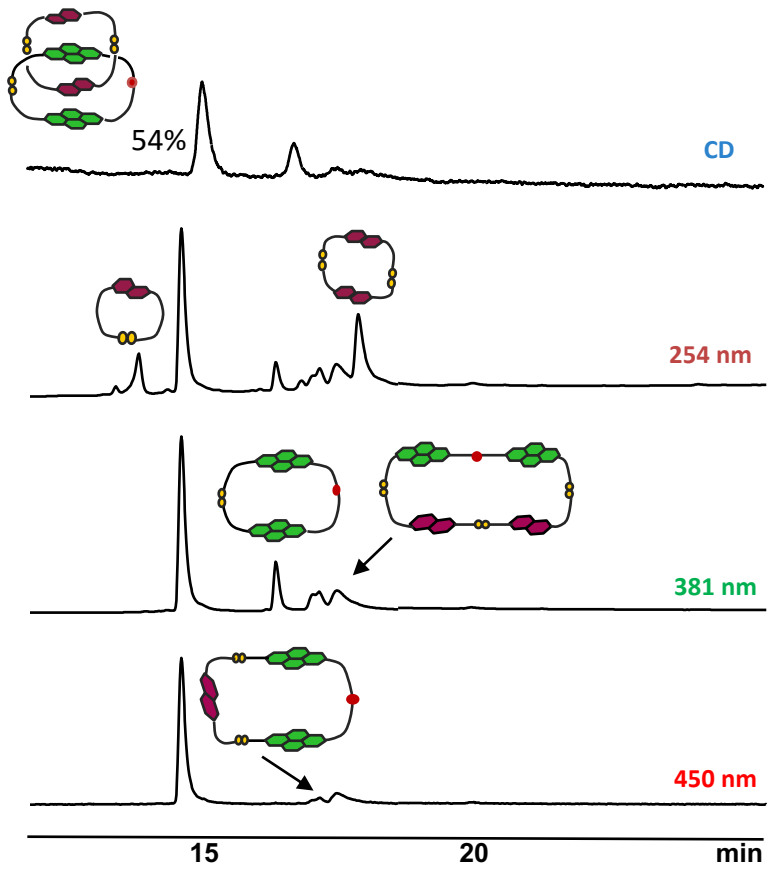

Figure S29. Effect of acetonitrile-water solvent mixture on the **A1*** and **D** library (1:1 ratio, 5 mM, H_2O, pH 8).

Kinetic Study of the Effect of CH_3CN : H_2O solvent on Formation of Catenane

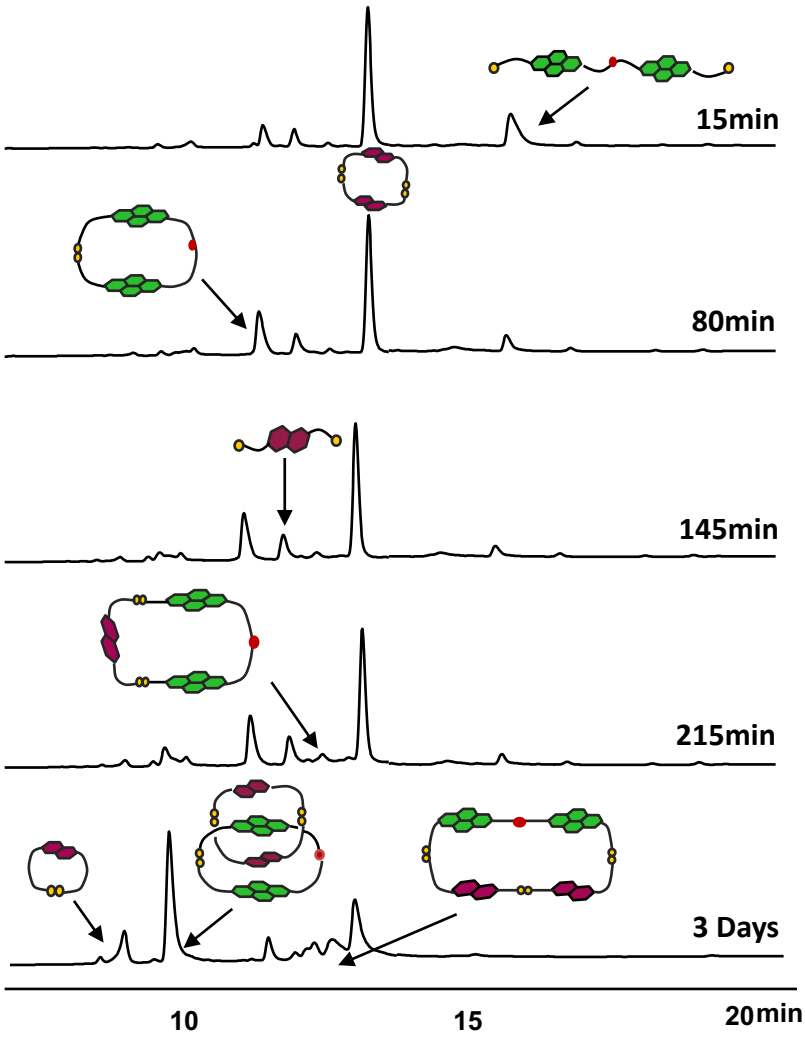

Figure S30. The kinetic study showing the gradual process of **A1*D$_2$** formation over time in acetonitrile-water solvent mixture. The kinetic of **A1*D$_2$** formation is slower in acetonitrile-water than only in water. Absorbance was monitored at 254 nm.

11. A2D$_2$: Analysis of the Species Present in the Library *via* HPLC

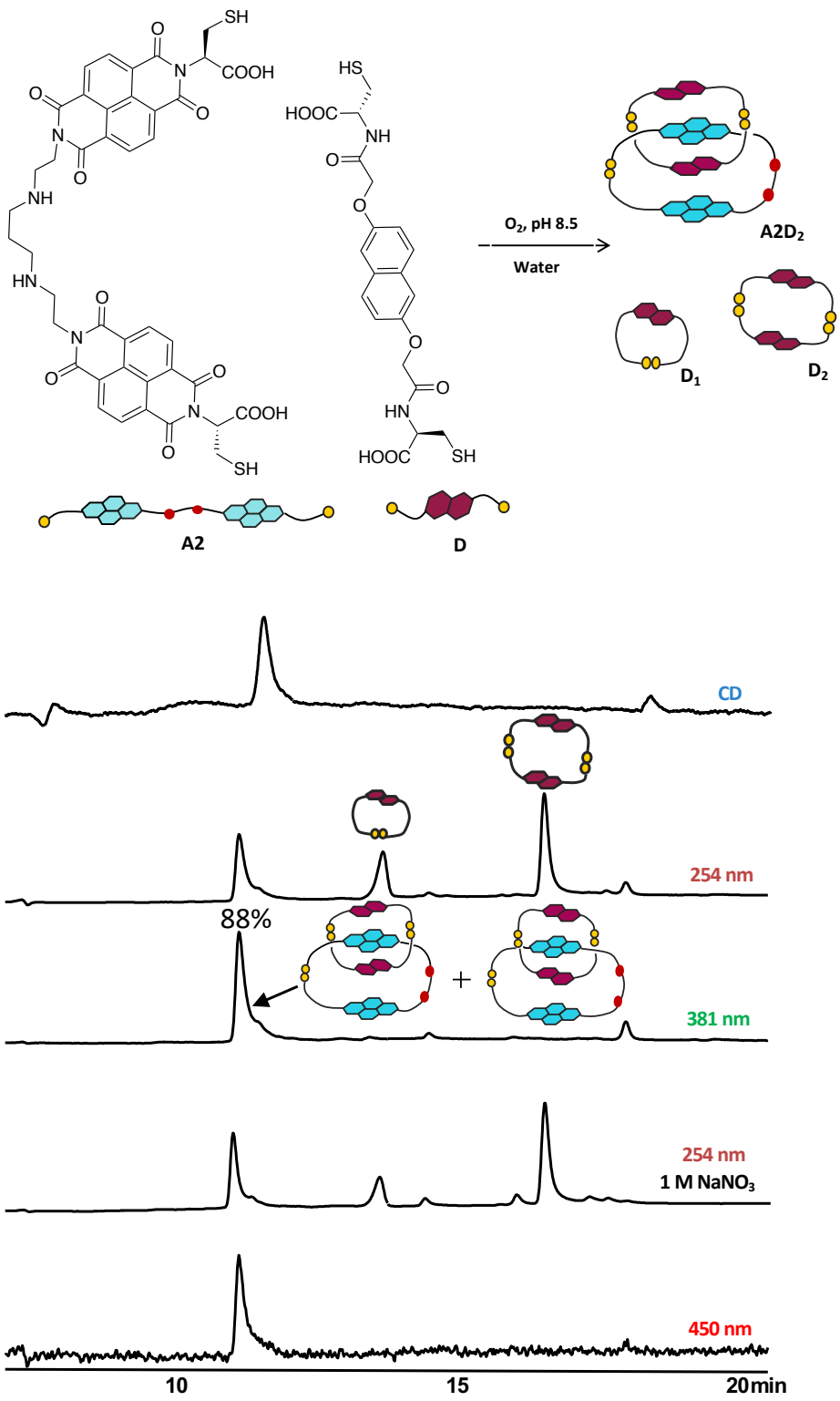

Figure S31. The HPLC analysis of D-A DCL of **A2** and **D** (1:2 molar ratio, 5 mM total concentration, H_2O).

LC-MS Analysis

MS spectra of the species identified in the aqueous library of **A2** with **D**.

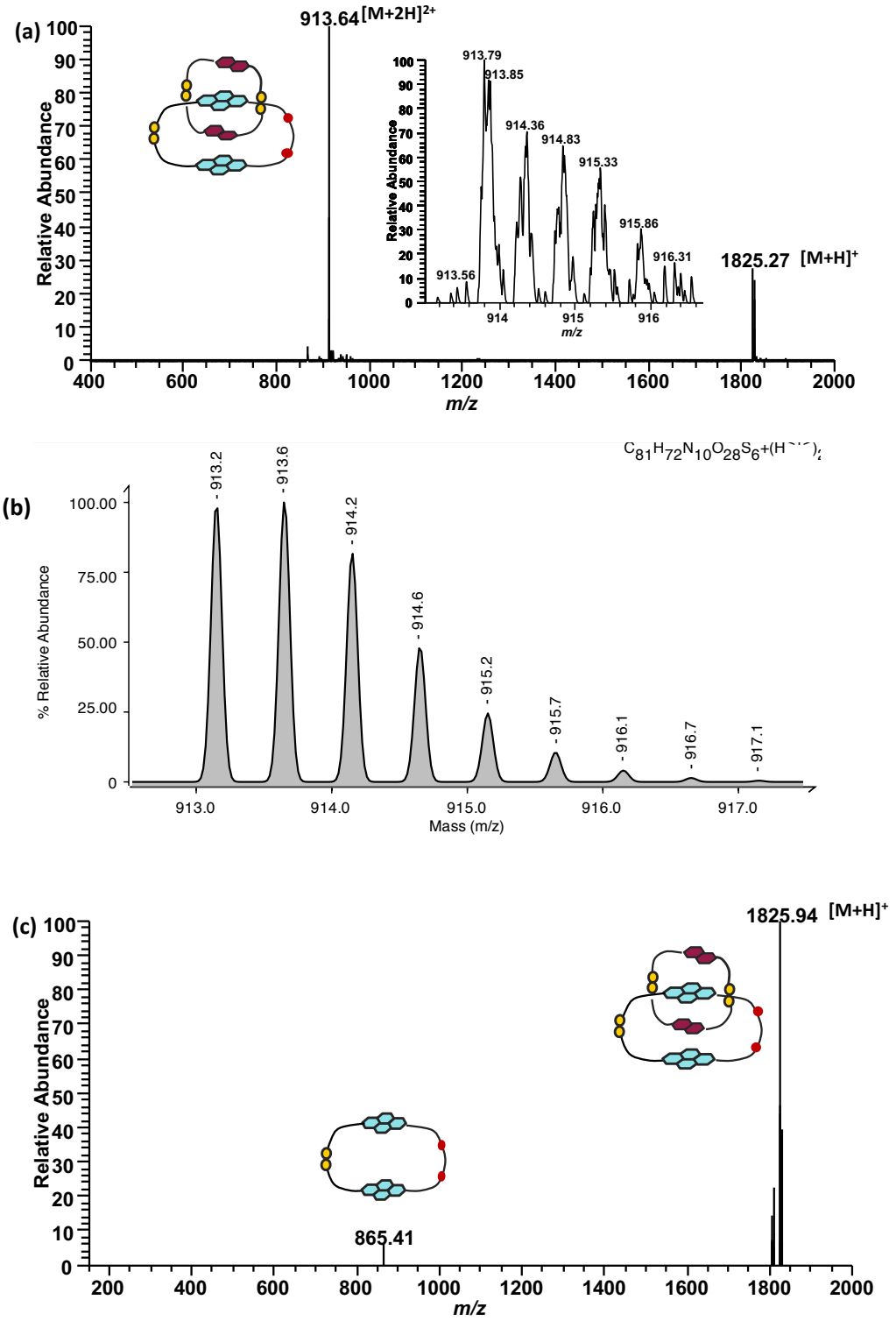

Figure S32. (a) ESI-MS (*+ve*), (b) Theoretical MS spectrum (*+ve*) and (c) MS/MS fragmentation of **A2D$_2$**. The ESI-MS and MS/MS results confirm the formation of **A2D$_2$**.

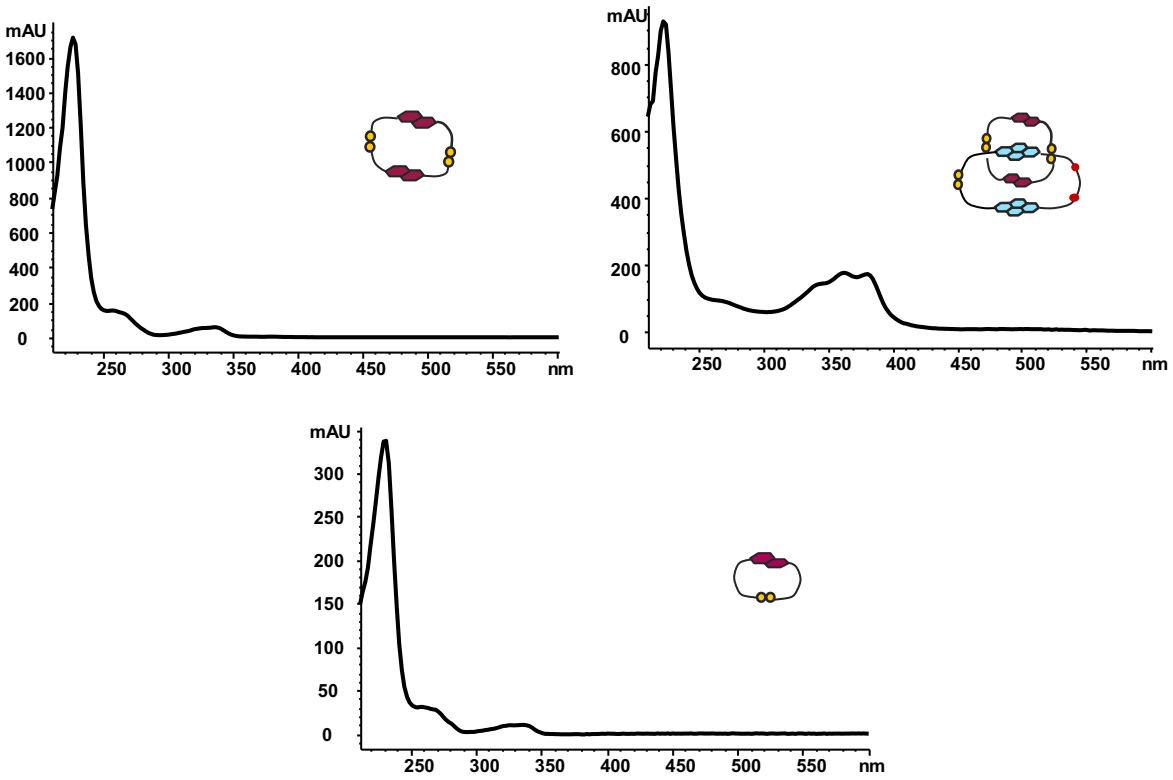

Figure S33. The UV-Vis spectrum of each peak and corresponding structure.

2-aminoethyl-1,3-propanediamine (**A2**) is a symmetrical polyamine and has two nitrogen atoms in the alkyl chain therefore the **A2D$_2$** catenane can have only two isomers.

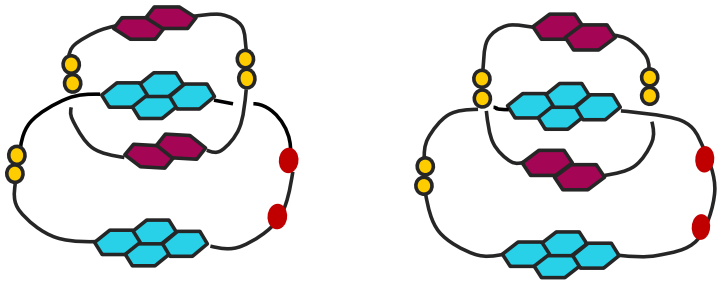

Figure S34. The possible DADA [2]catenane structures with **A2** and **D** building block.

12. 1D and 2D ^{1}H NMR Analysis

In order to confirm that the peak at 8.5 min is a [2]catenane and not a macrocycle, it was isolated by preparative HPLC (isolated yield: 92%, Figure S35) and analysed by NMR.

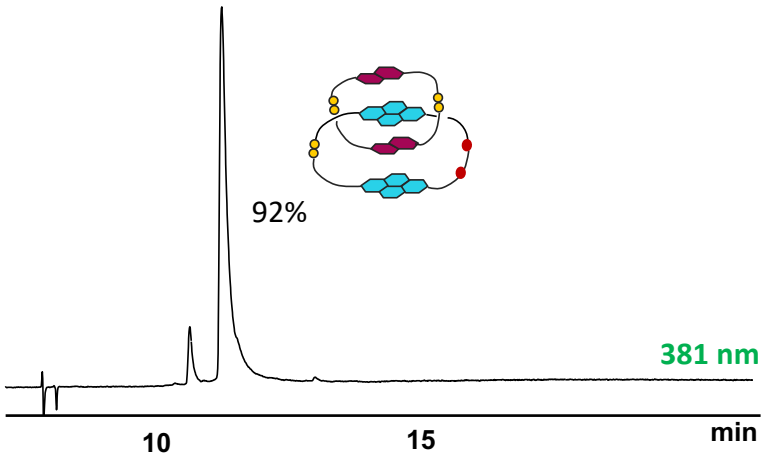

Figure S35. Reverse-Phase HPLC result of the isolated **A2D$_2$** catenane. Absorbance was recorded 381 nm.

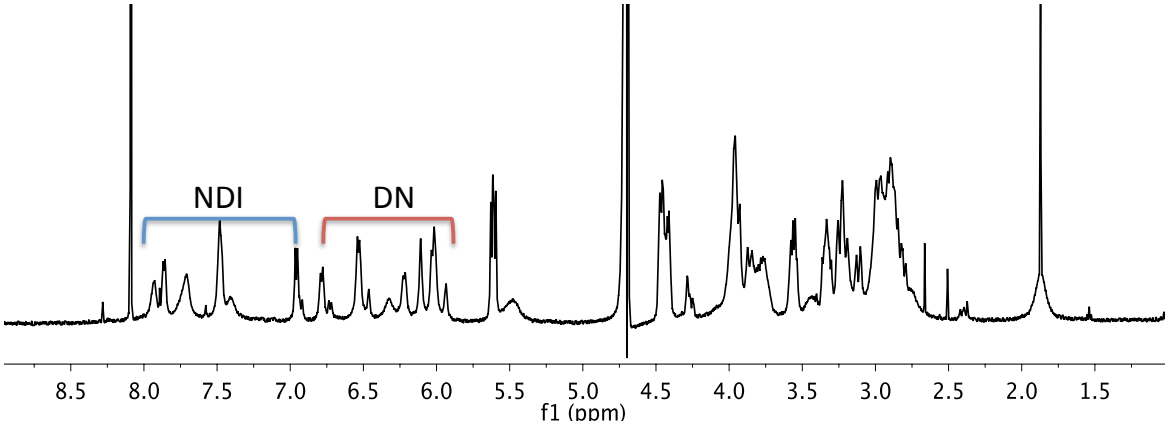

Figure S36. ^{1}H NMR Full spectrum of **A2D$_2$** catenane (D_2O, 500 MHz). The solvent peak was referenced at 4.74 ppm.

The catenated nature of **A2D$_2$** was confirmed by NMR spectroscopy by the upfield NMR signals of the NDI and DN regions in D_2O Figure S36 (500 MHz) which is an indication of aromatic stacking and also the sharp nature of the signals indicates rigidity through complex topology. Distinctively macrocycles usually give very broad NMR signals due to their flexibility.

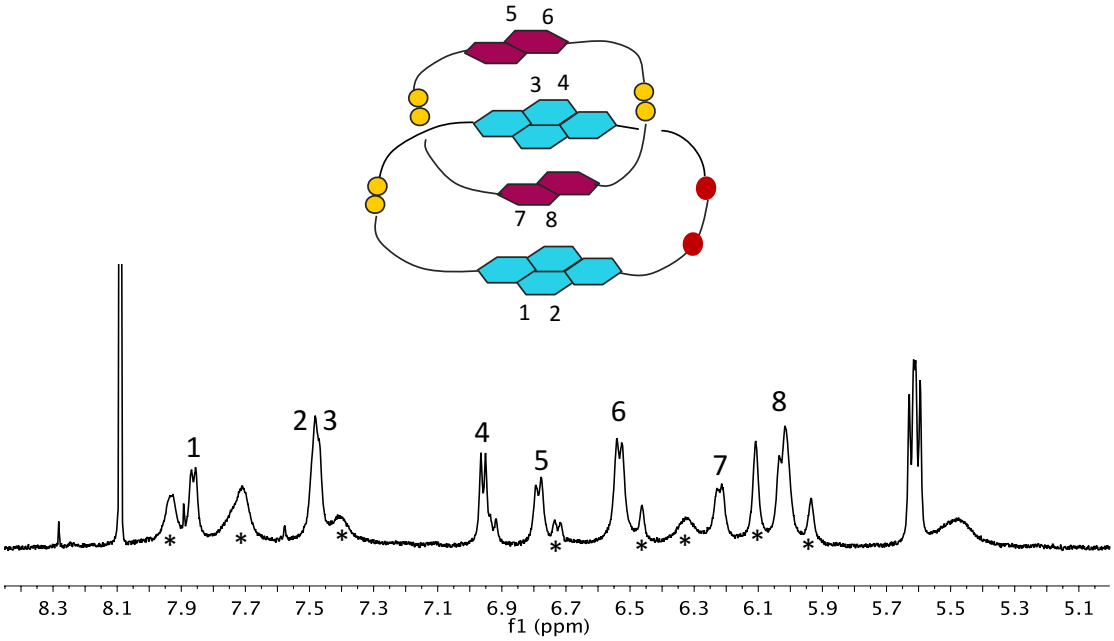

Figure S37. ^{1}H NMR spectrum of **A2D$_2$** catenane from 5.0 – 8.4 ppm. The solvent peak was referenced at 4.74 ppm.

The ^{1}H NMR of **A2D$_2$** is consequently simpler that what we observed for **A1D$_2$**, since there are only two catenanes formed. However, by the COSY analysis of the donor and acceptor regions, the correlation was very weak and not all the peaks could be identified (represented by *).

The aromatic region of the ^{1}H NMR spectrum displays the peaks corresponding to two diastereomers, which have the characteristic upfield shifts for the stacked NDI and DN moieties (7.9 – 6.7 ppm for NDI and 6.8 – 5.9 ppm for DN; Figure S37). The ^{1}H NMR spectrum indicates that one of the two diastereomers is more conformationally flexible as suggested by the broad signals associated to this structure, which can be explained by the longer linker in between the NDI cores in **A2D$_2$** when compared to **A1D$_2$**.

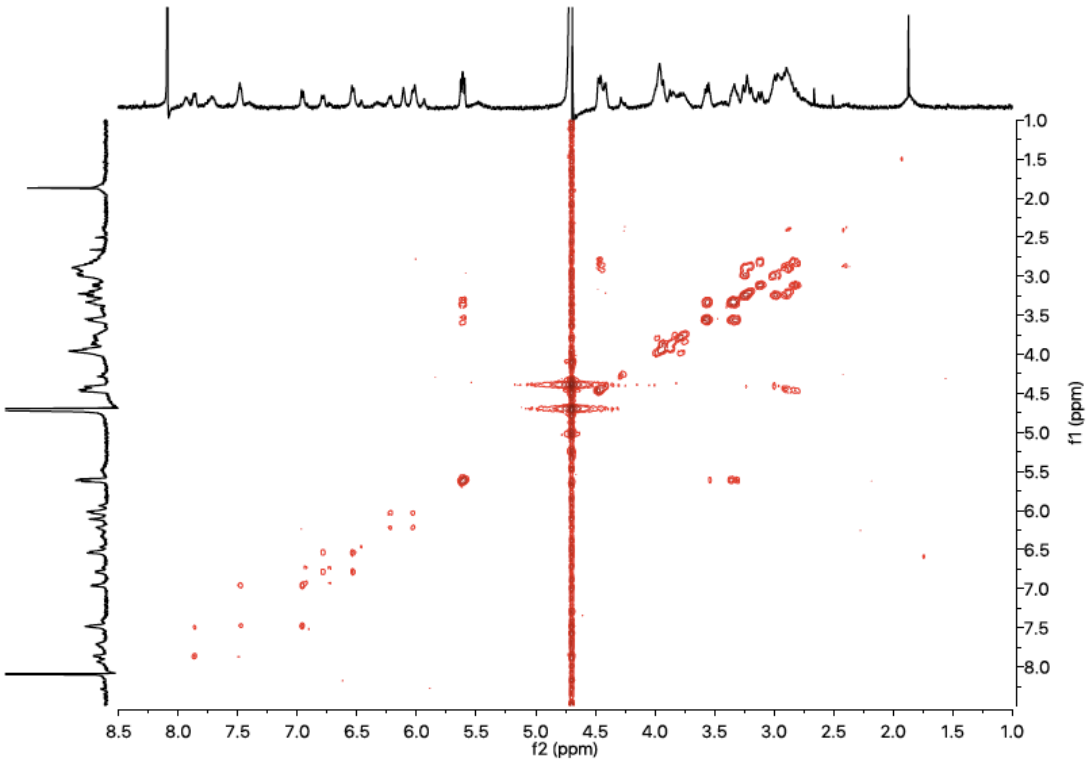

Figure S38. Full COSY spectrum of **A2D$_2$** catenane (D_2O, 500 MHz). The solvent peak was referenced at 4.74 ppm.

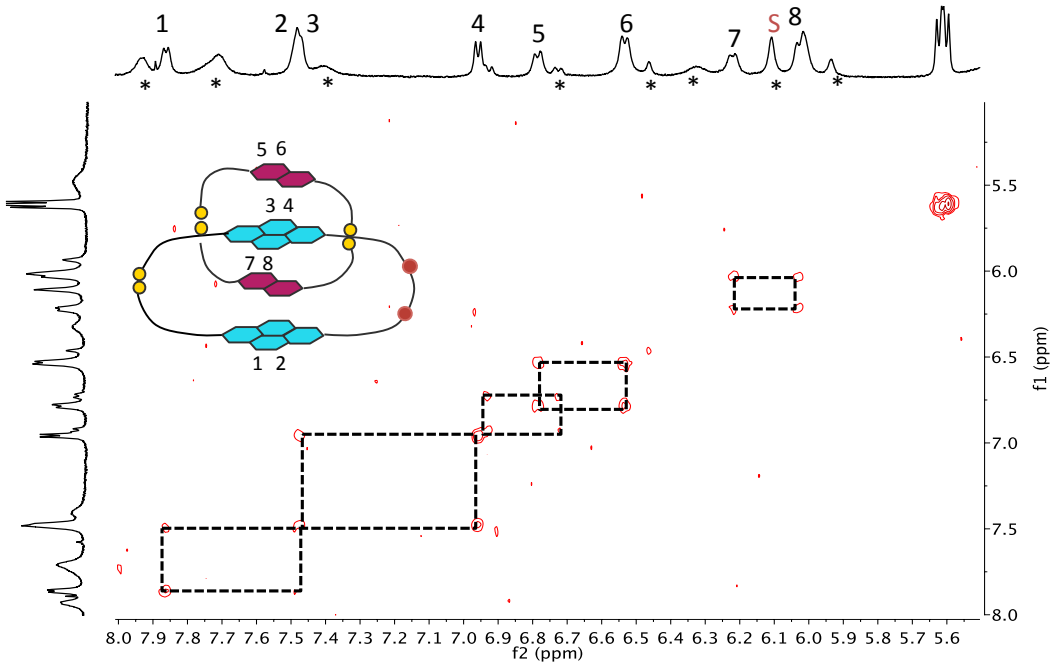

Figure S39. Partial COSY spectrum of **A2D$_2$** catenane between 5.5 – 8.0 ppm (D_2O, 500 MHz). The solvent peak was referenced at 4.74 ppm. **S** = represents the singlet peak of the dialkoxynphthalene.

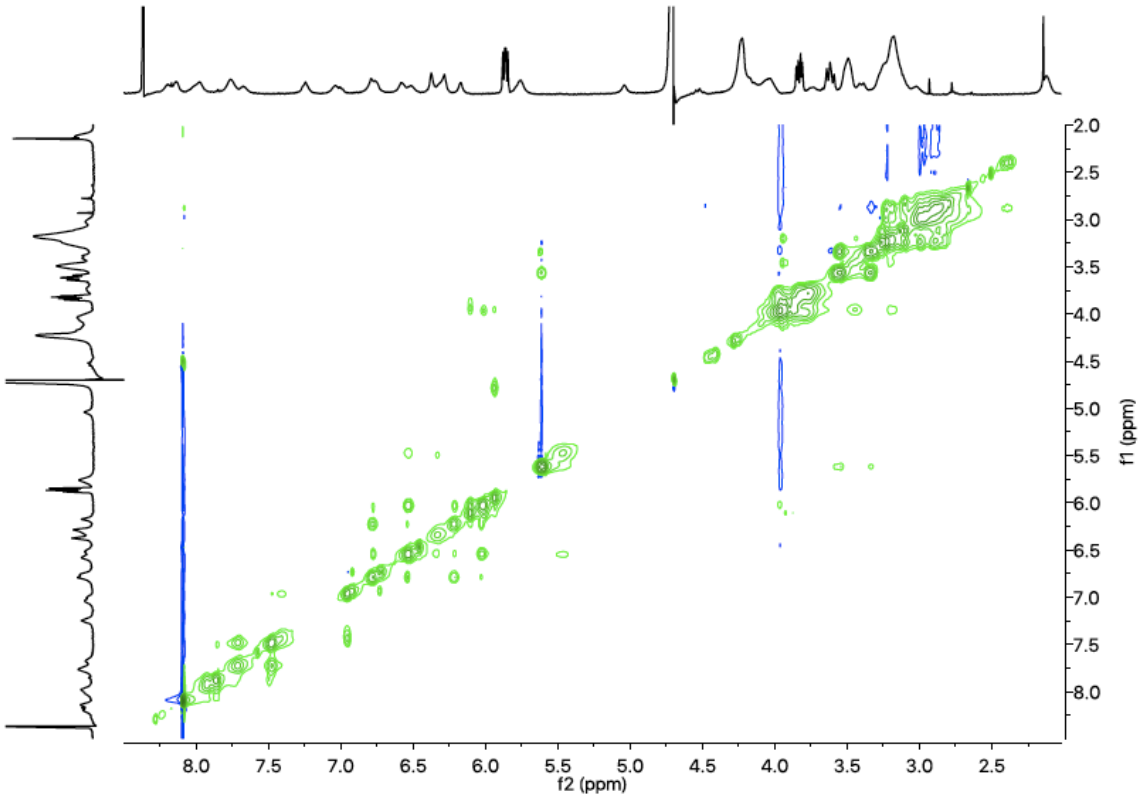

Figure S40. Full NOESY spectrum of **A2D$_2$** catenane (D_2O, 500 MHz).

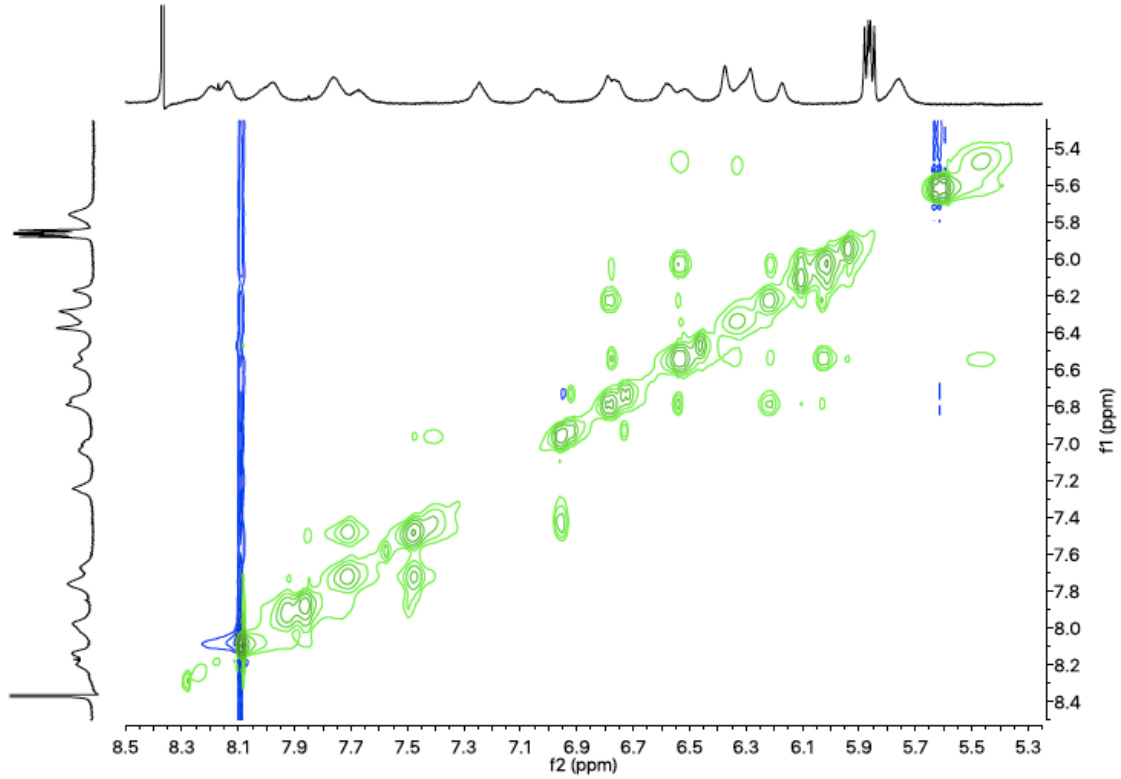

Figure S41. Partial NOESY spectrum of **A2D$_2$** catenane from 5.2 – 8.50 ppm (D_2O, 500 MHz).

13. Circular Dichroism (CD) Analysis

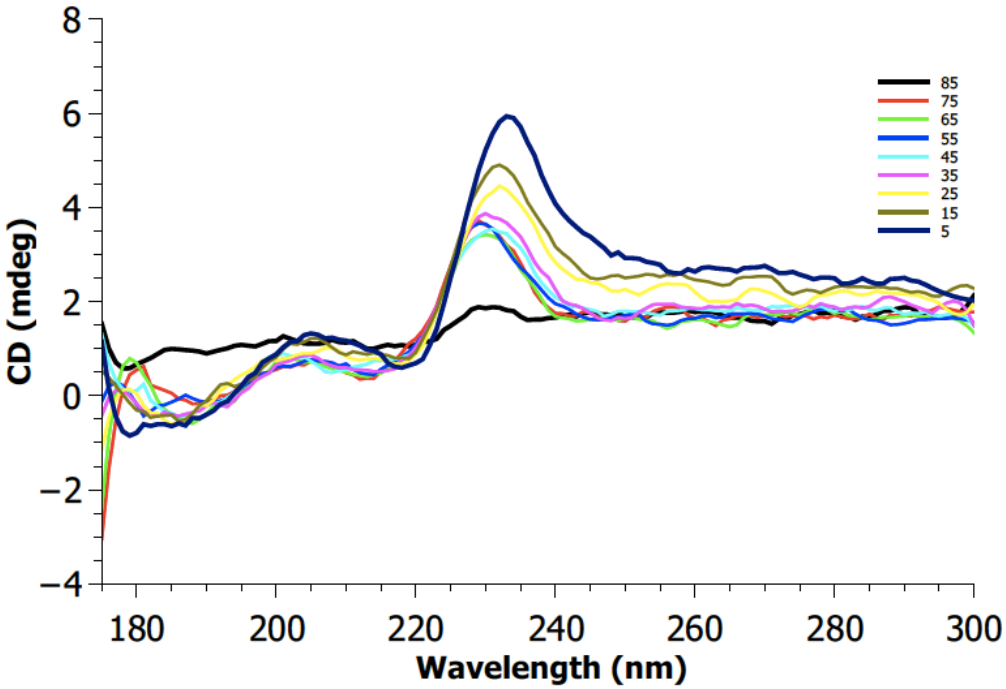

Figure S42. Variable temperature CD spectra between 5 – 85 °C of **A2D$_2$** (D_2O, 175 – 300 nm, 1 mm cuvette pathlength).

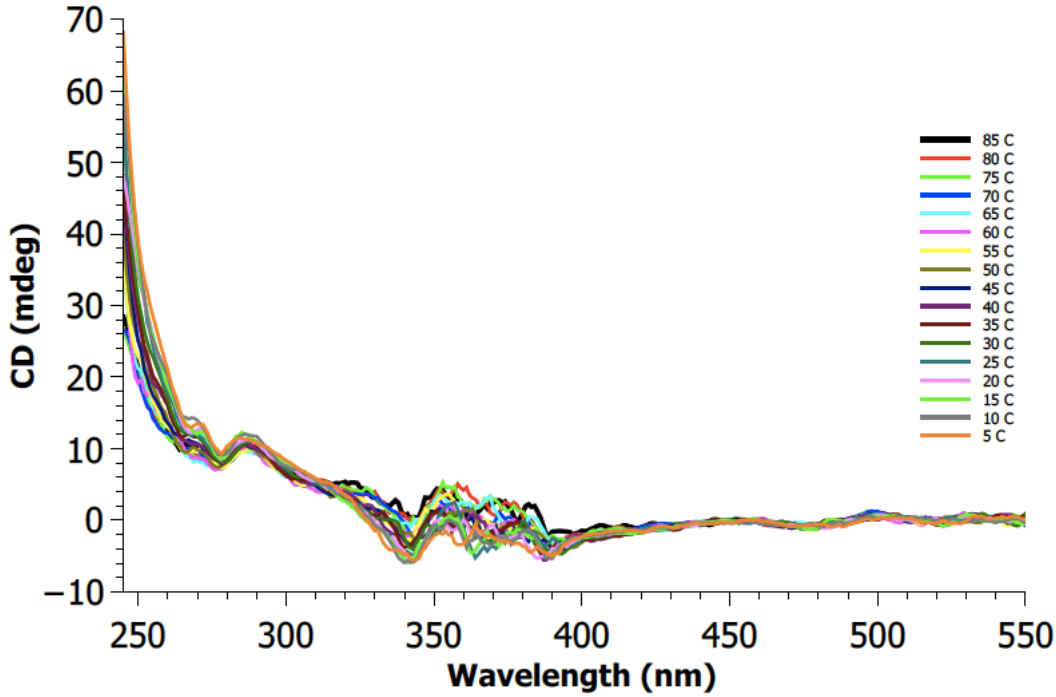

Figure S43. Variable temperature CD spectra between 5 – 85 °C of **A2D$_2$** (D_2O, 245 – 550 nm, 10 mm cuvette pathlength).

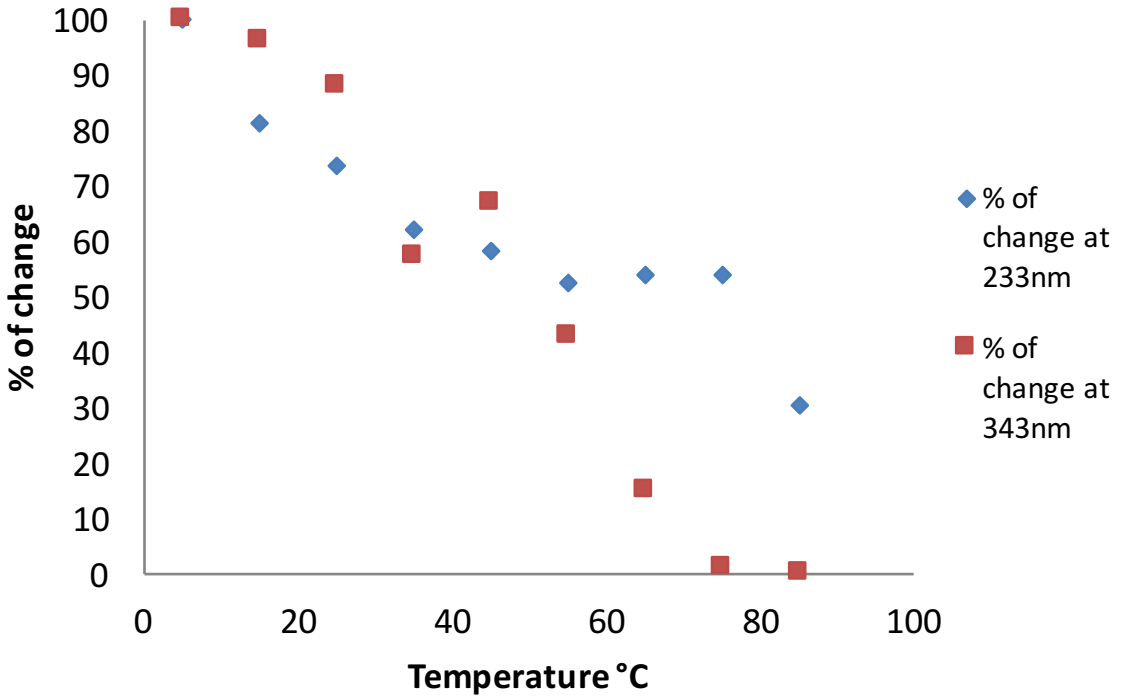

Figure S44. The comparison between % of change in two wavelengths (233 and 343 nm) of **A2D$_2$**. This catenane, is more flexible in the NDI region, higher wavelength, (343 nm) than in the cysteine region.

14. The Effect of Chirality on Catenane Formation

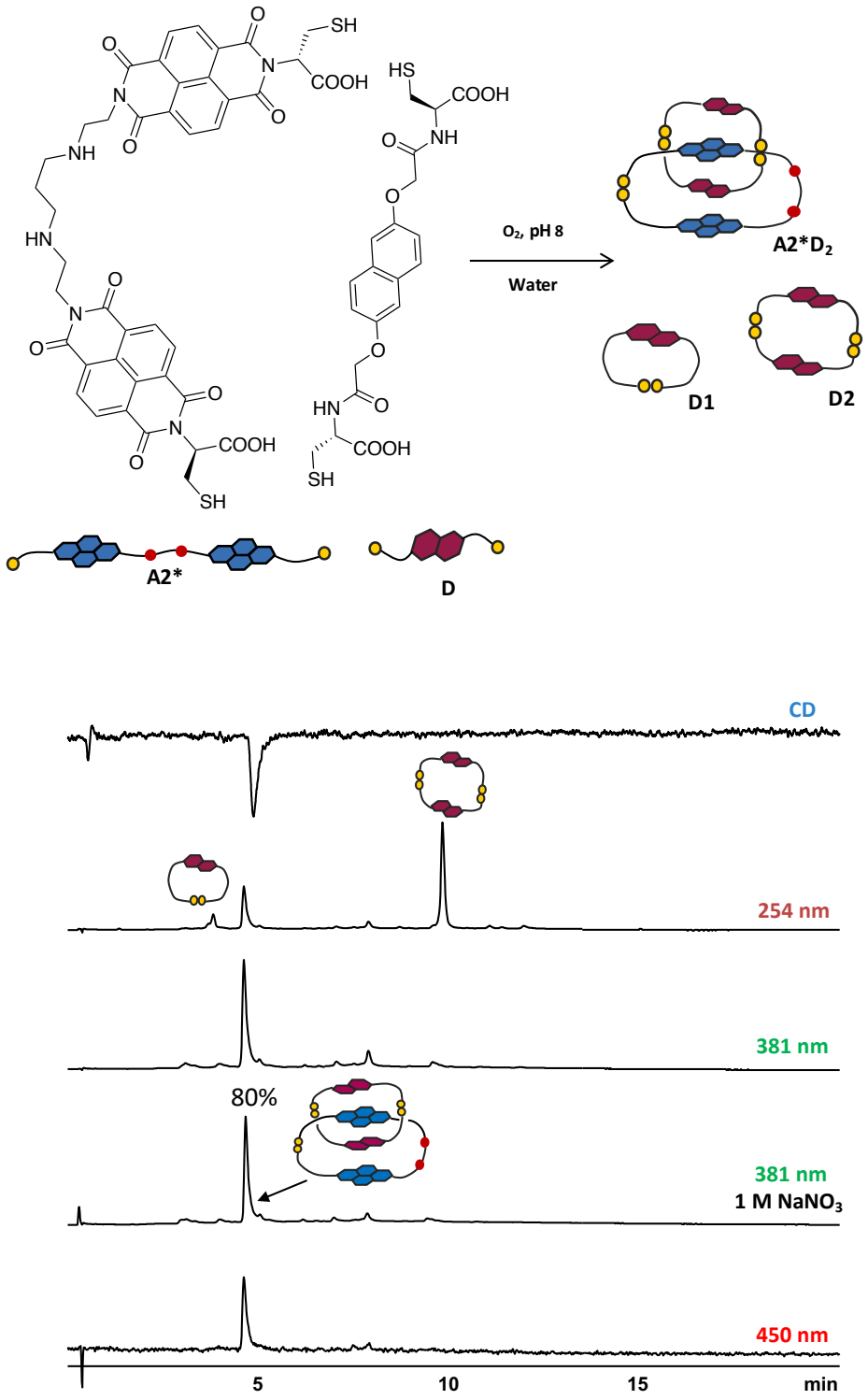

Figure S45. The HPLC analysis of D-A DCL of **A2*** and **D** (1:2 molar ratio, 5 mM total concentration, H_2O).

Changing the point chirality of the **A2** building block from L to D on the cysteine appendages does not affect significantly the DCL's distribution.

Kinetics of A2*D_2 Formation

The kinetic study showing the formation of **A2*D_2** over time. The number of intermediates and macrocyclic species is higher at the beginning of library, and it starts to decrease to three species as the library reaches equilibrium.

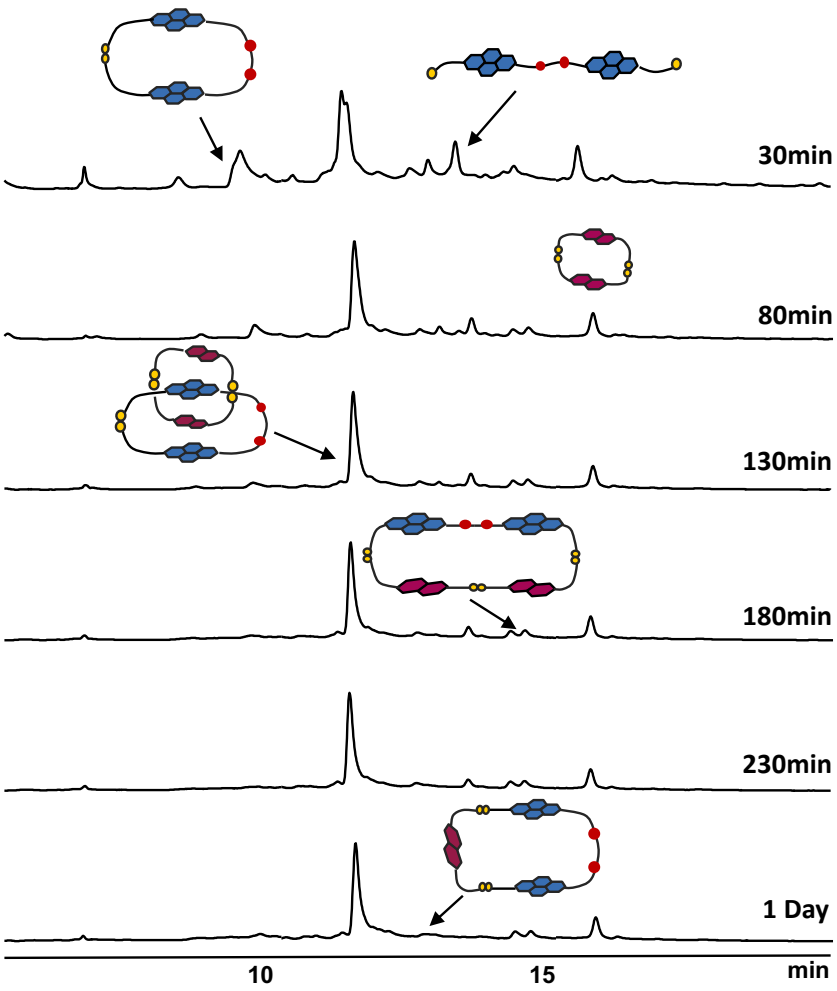

Figure S46. Kinetic study showing the formation of **A2*D_2** over time. The absorbance was recorded at 381 nm.

LC-MS Analysis

MS spectra of the species identified in the aqueous library of **A2*** with **D**.

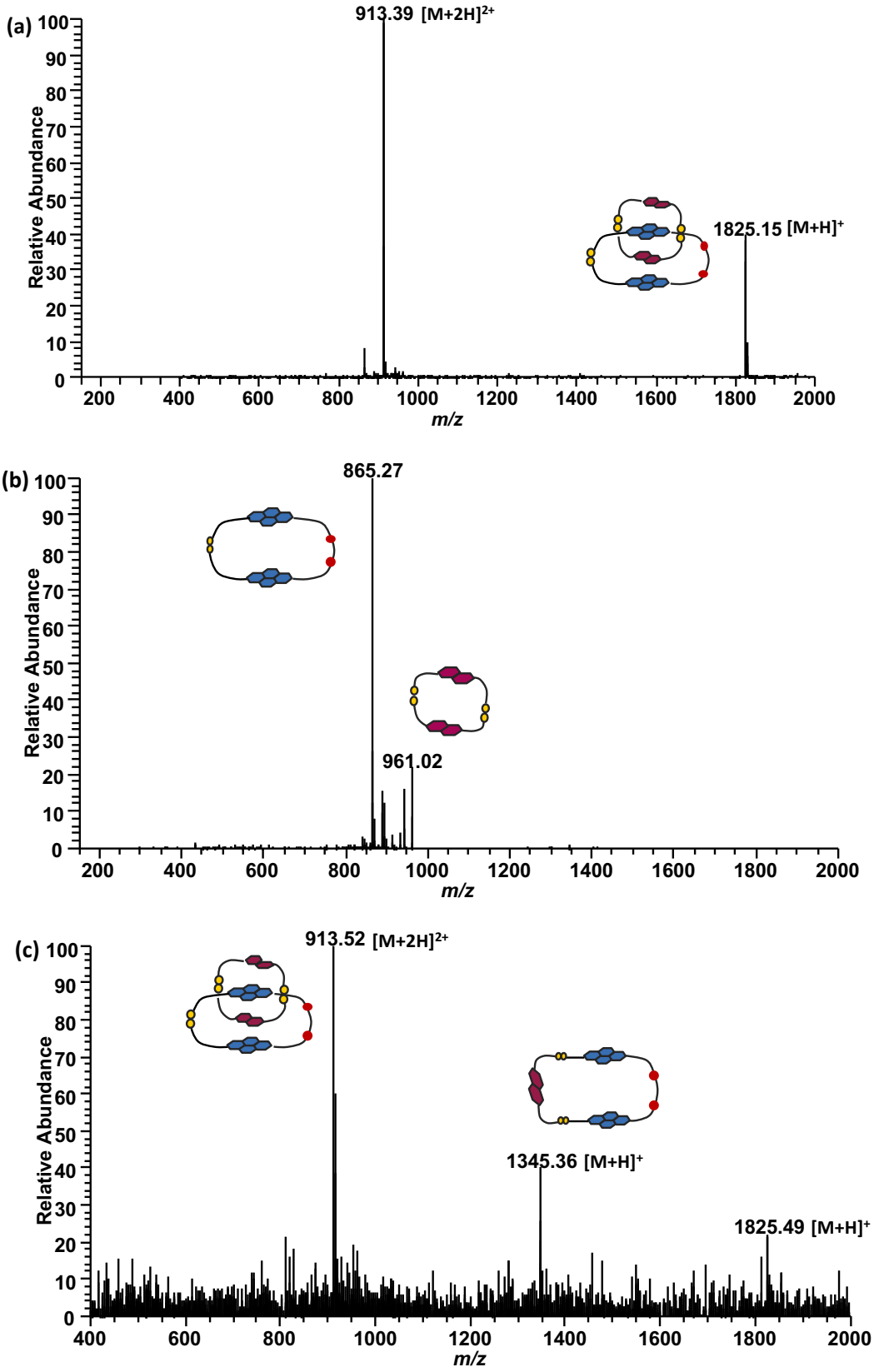

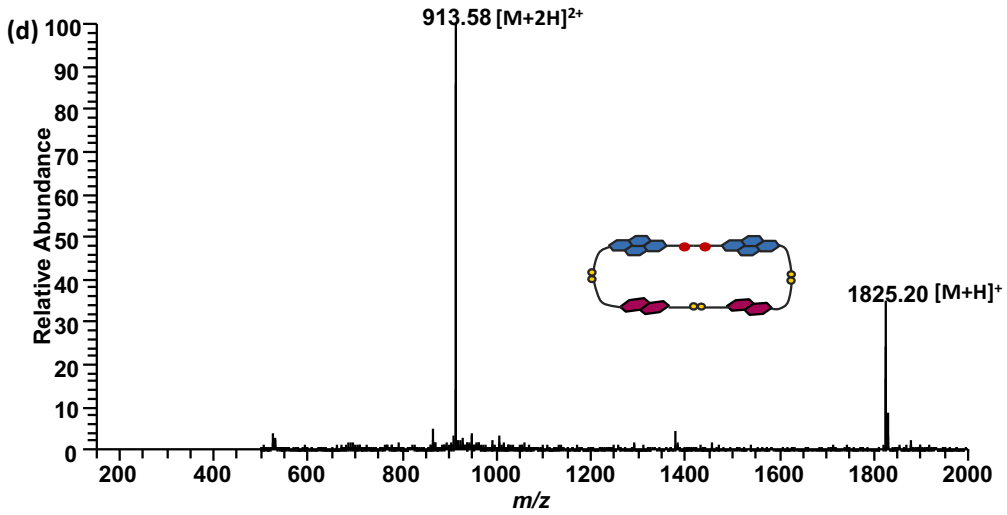

Figure S47. (a) Full MS (*+ve*) and (b) MS/MS fragmentation of **A2*D$_2$**, (c) Full MS (*+ve*) of heterodimer of **A2*** and **D**, (d) Full MS (*+ve*) of cyclic heterotrimer of **A2*D$_2$**. The ESI-MS and MS/MS results confirm the formation of different moieties in **A2*** and **D** library.

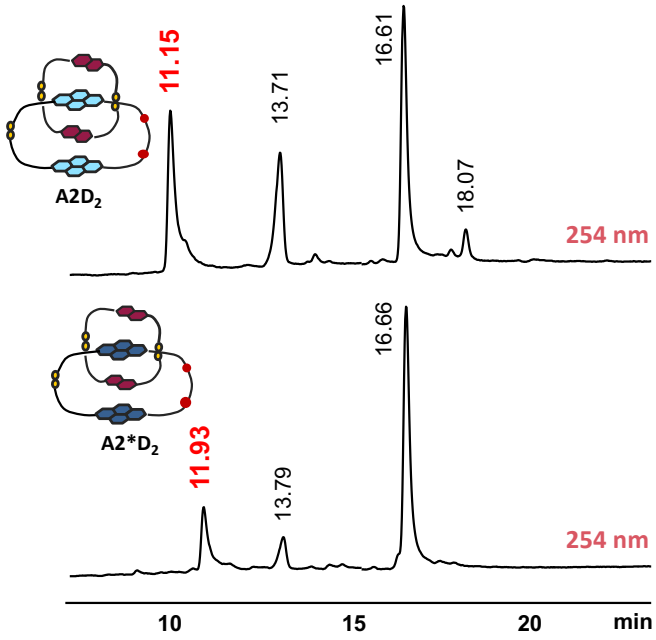

Figure S48. The comparison between the HPLC traces of **A2D$_2$** and **A2*D$_2$** (on the same condition and same column).

As with the **A1D$_2$** / **A1*D$_2$** pair, the change in point chirality has a slight influence on the retention time of the isomeric **A2D$_2$** / **A2*D$_2$** [2]catenanes, which elute at 11.15 and 11.93 min, respectively under identical HPLC conditions.

15. Circular Dichroism (CD) analysis

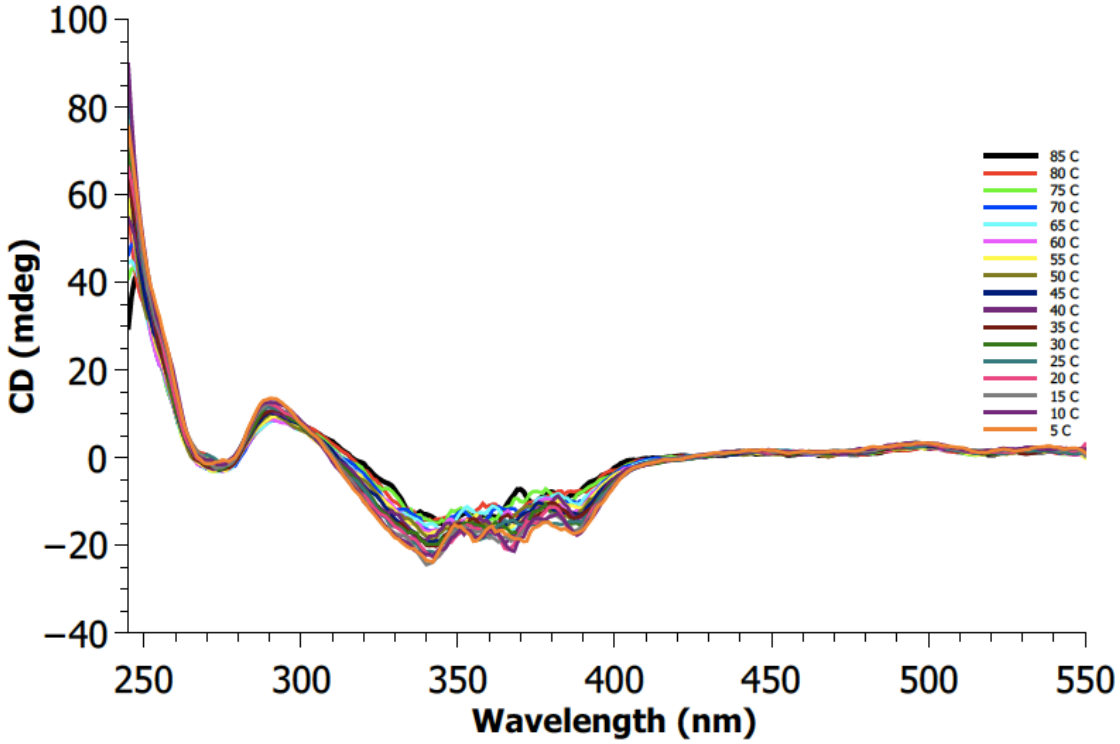

Figure S49. Variable temperature CD spectra between 5 – 85 °C of **A2*D$_2$** (D_2O, 245 – 550 nm, 10 mm cuvette pathlength).

16. ^{1}H and ^{13}C NMR

A1 Protected

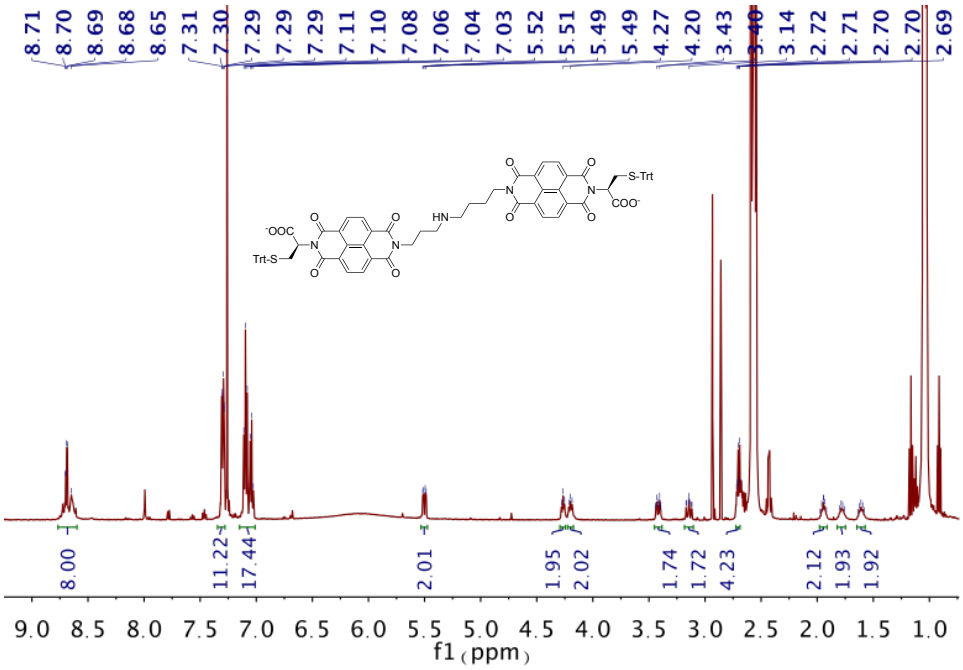

Figure S50. ^{1}H NMR of **A1** building block. The peaks that have been integrated correspond to compound **A1**; the peaks that have not been integrated correspond to solvent impurities such as DMF and Et_3N.

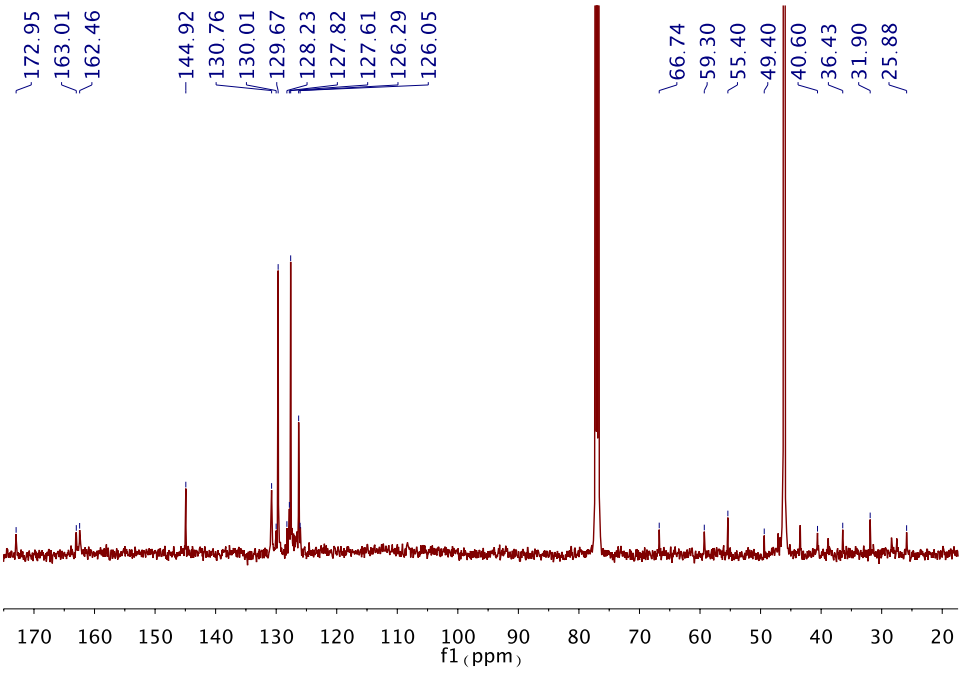

Figure S51. ^{13}C NMR of **A1** protected building block.

A1 Deprotected

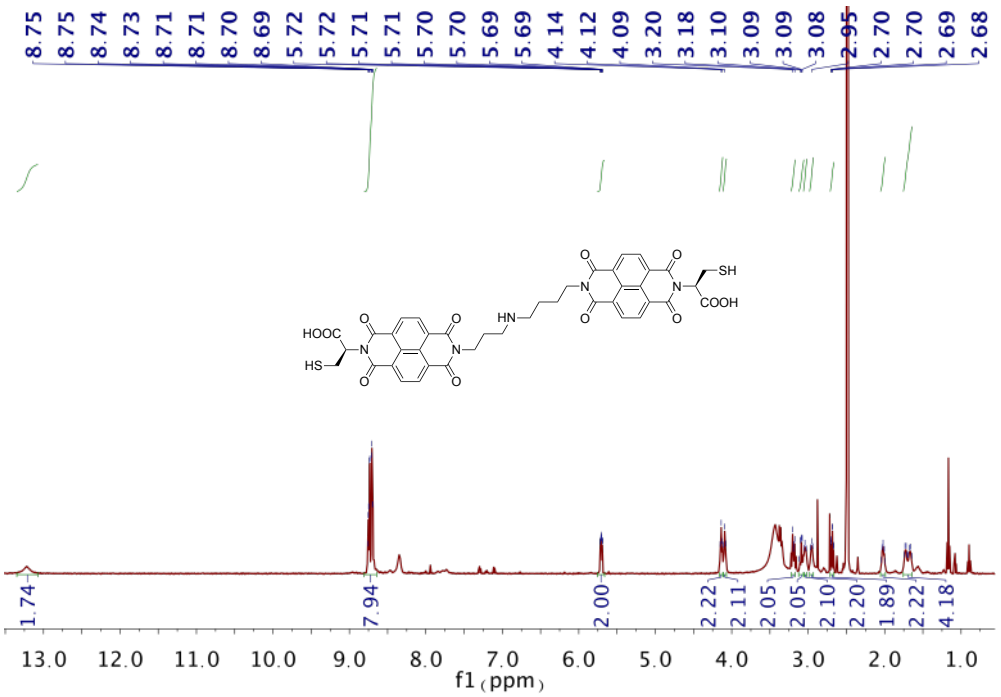

Figure S52. ^{1}H NMR of **A1** deprotected. The peaks that have not been integrated correspond to solvent impurities.

A1* Protected

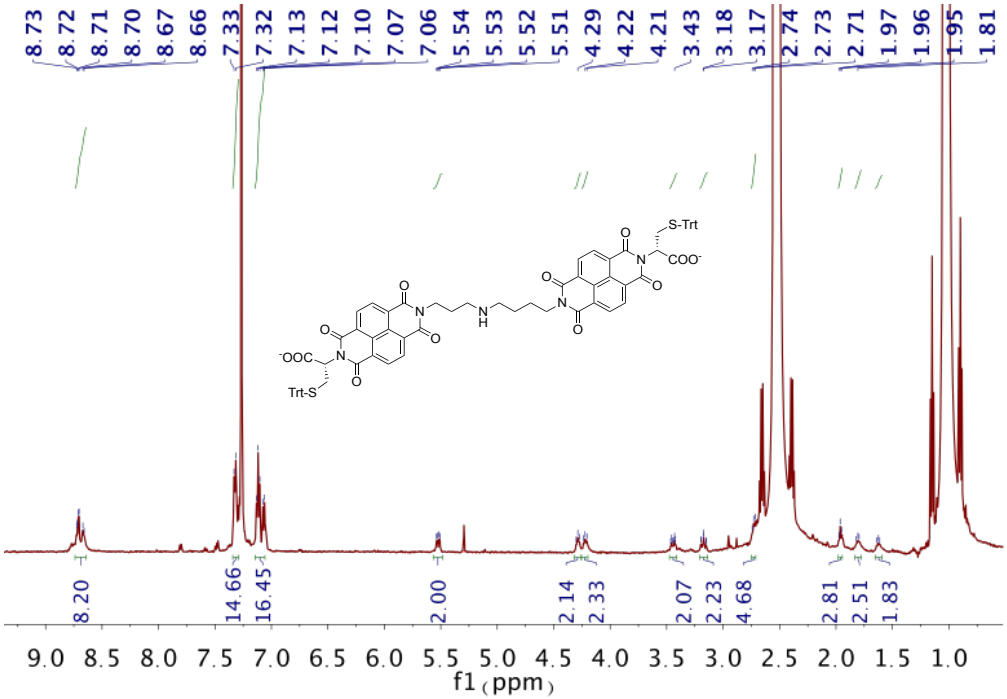

Figure S53. ^{1}H NMR of **A1*** building block. The peaks that have not been integrated correspond to solvent impurities such as DMF and Et_3N.

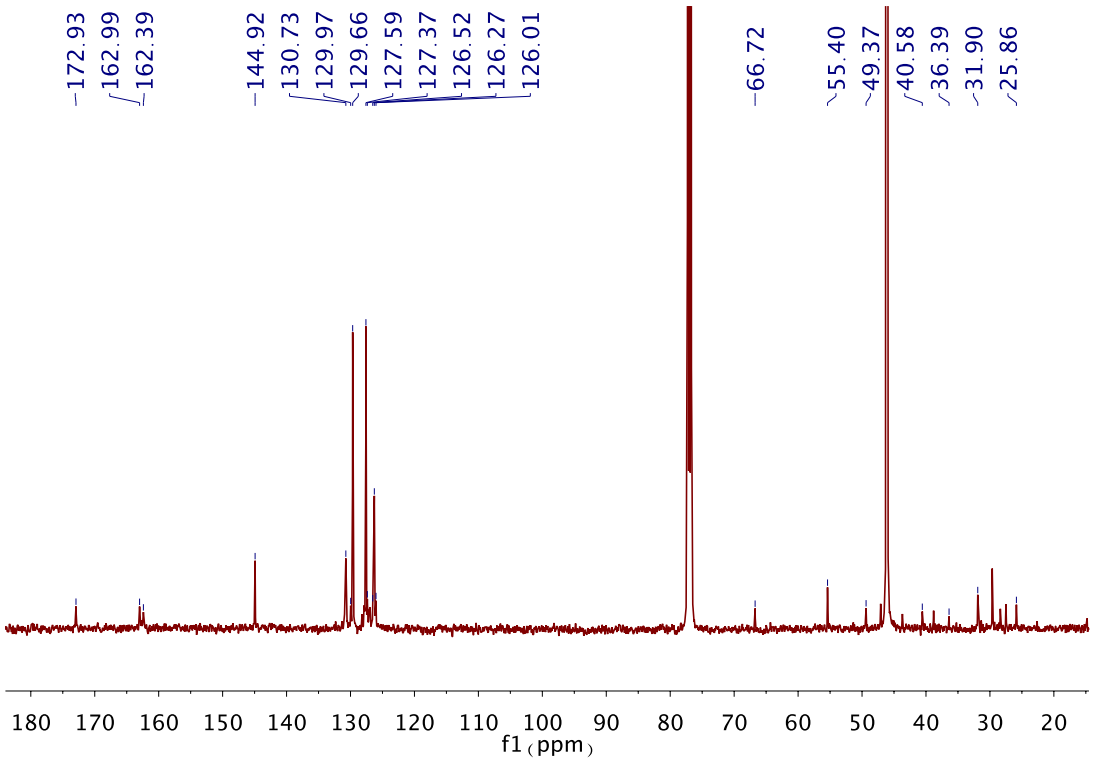

Figure S54. ^{13}C NMR of **A1*** building block.

A1* Deprotected

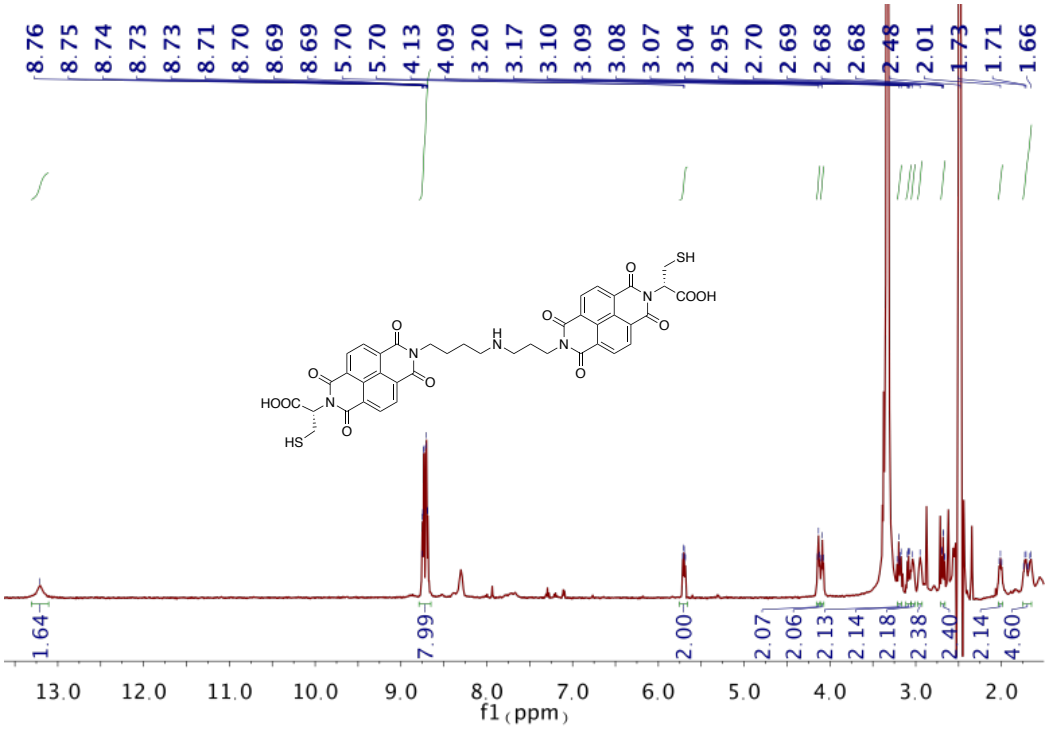

Figure S55. ^{1}H NMR of **A1*** deprotected. The peaks that have not been integrated correspond to solvent impurities.

A2 Protected

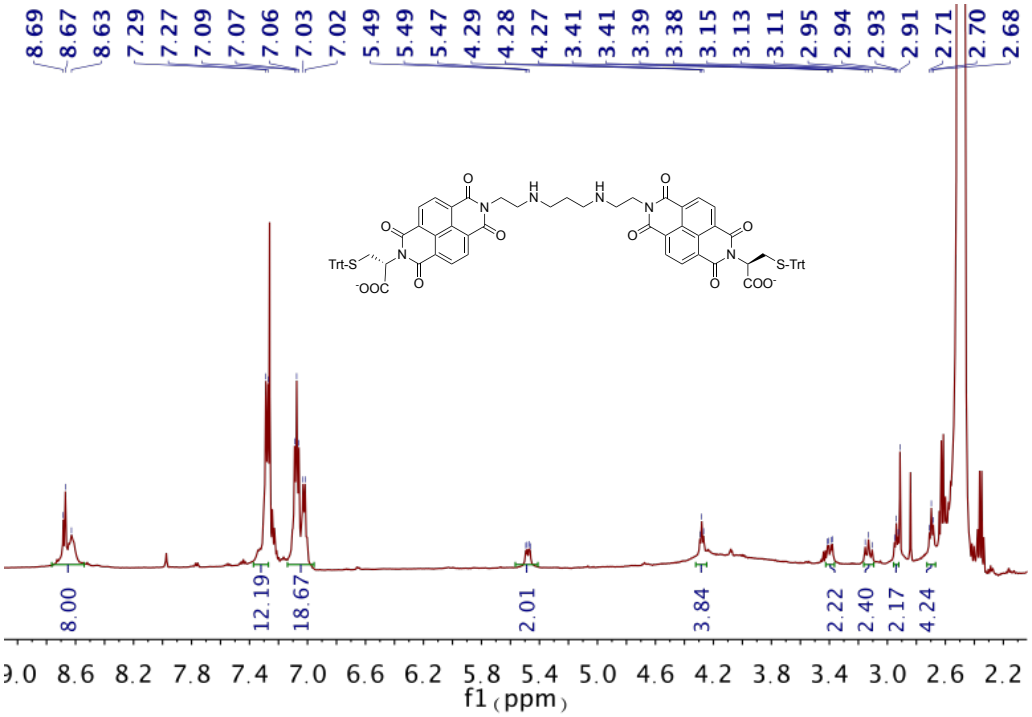

Figure S56. ^{1}H NMR of **A2** building block. The peaks that have not been integrated correspond to solvent impurities such as DMF and Et_3N.

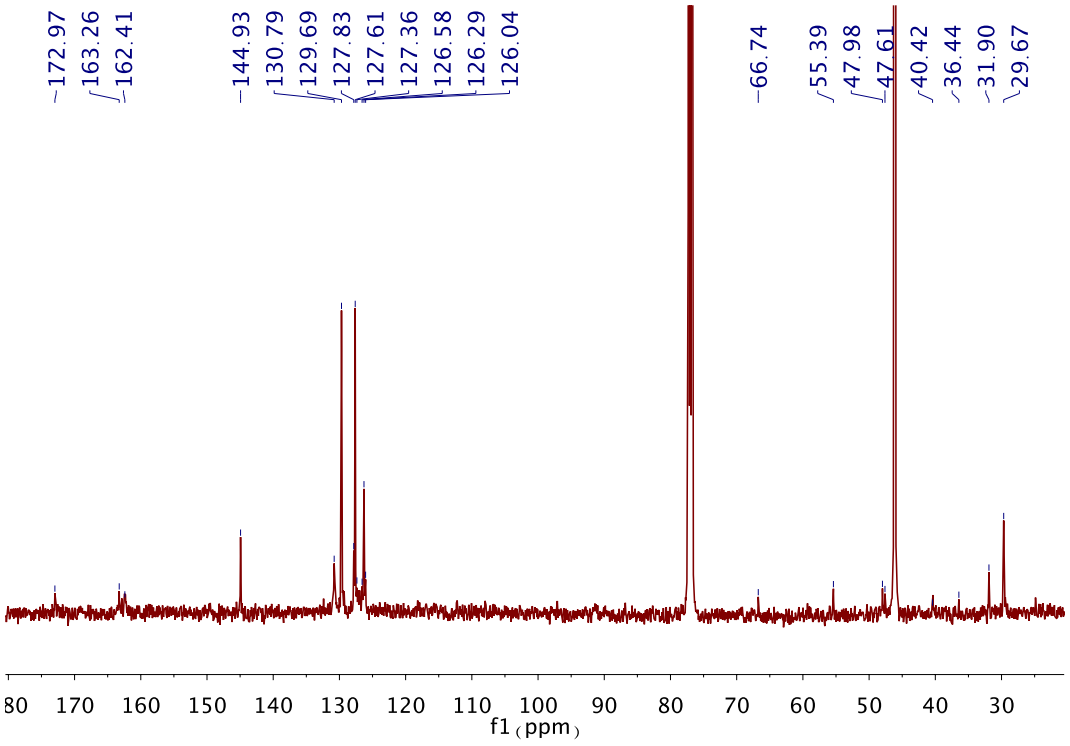

Figure S57. ^{13}C NMR of **A2** building block.

A2 Deprotected

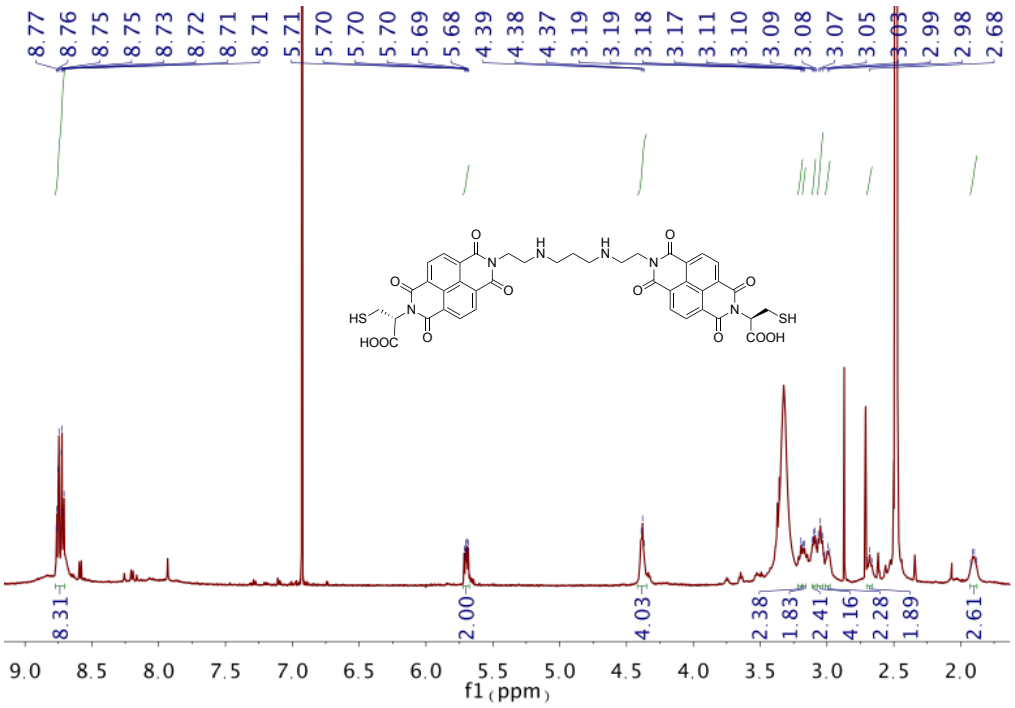

Figure S58. ^{1}H NMR of **A2** deprotected. The peaks that have not been integrated correspond to solvent impurities such as water and DMF.

A2* Protected

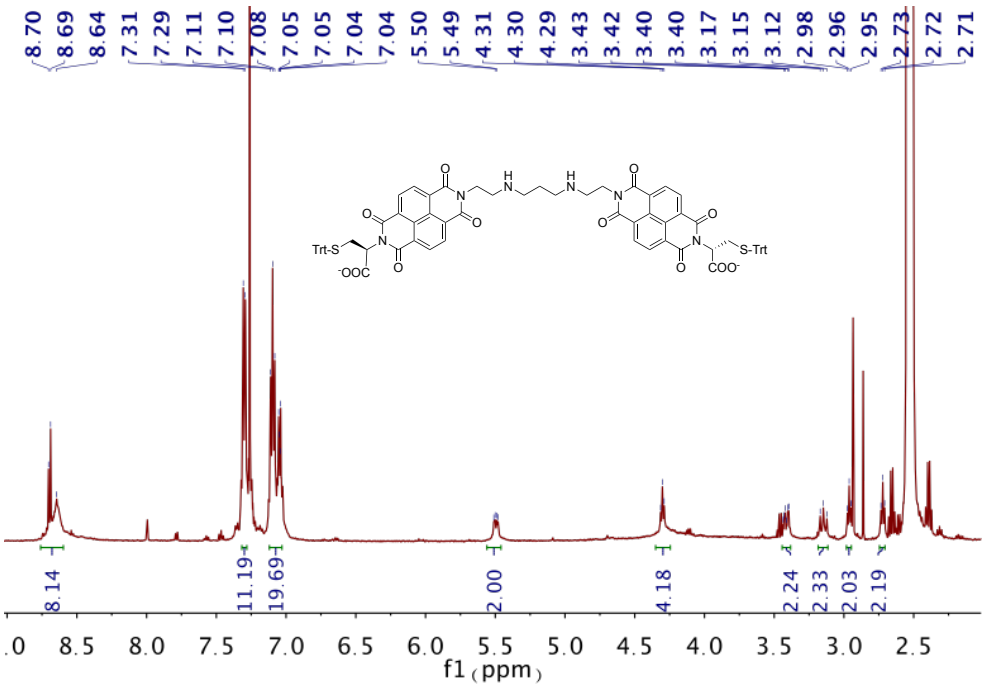

Figure S59. ^{1}H NMR of **A2*** building block. The peaks that have not been integrated correspond to solvent impurities such as DMF and Et_3N.

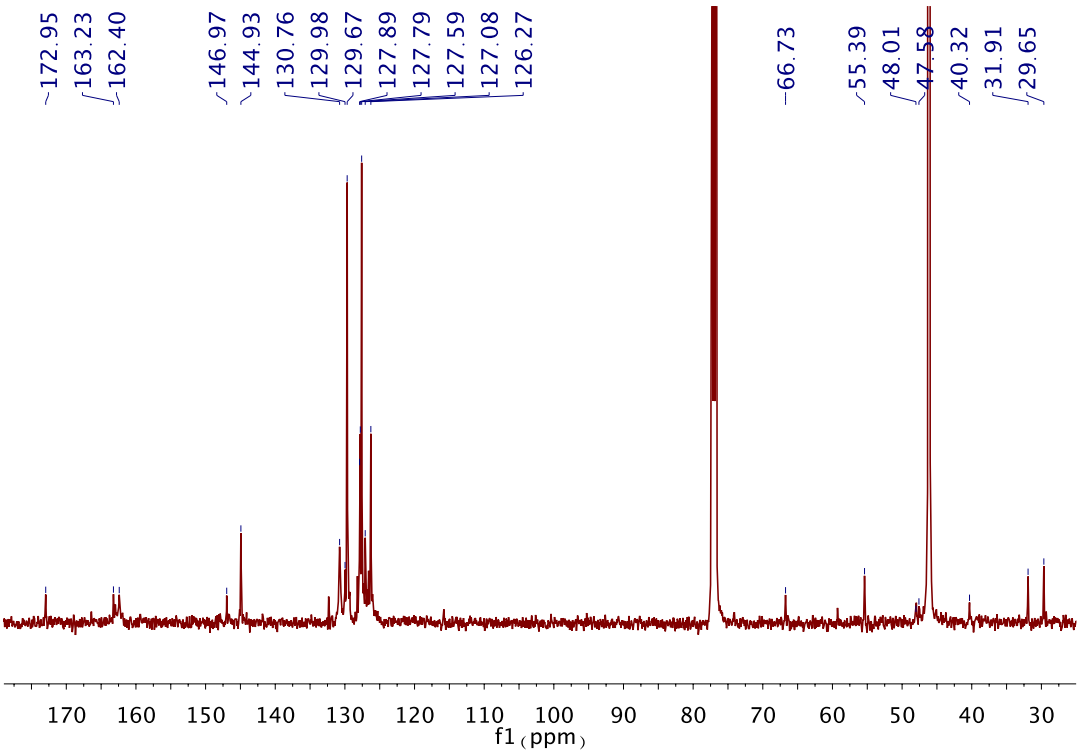

Figure S60. ^{13}C NMR of **A2*** building block.

A2* Deprotected

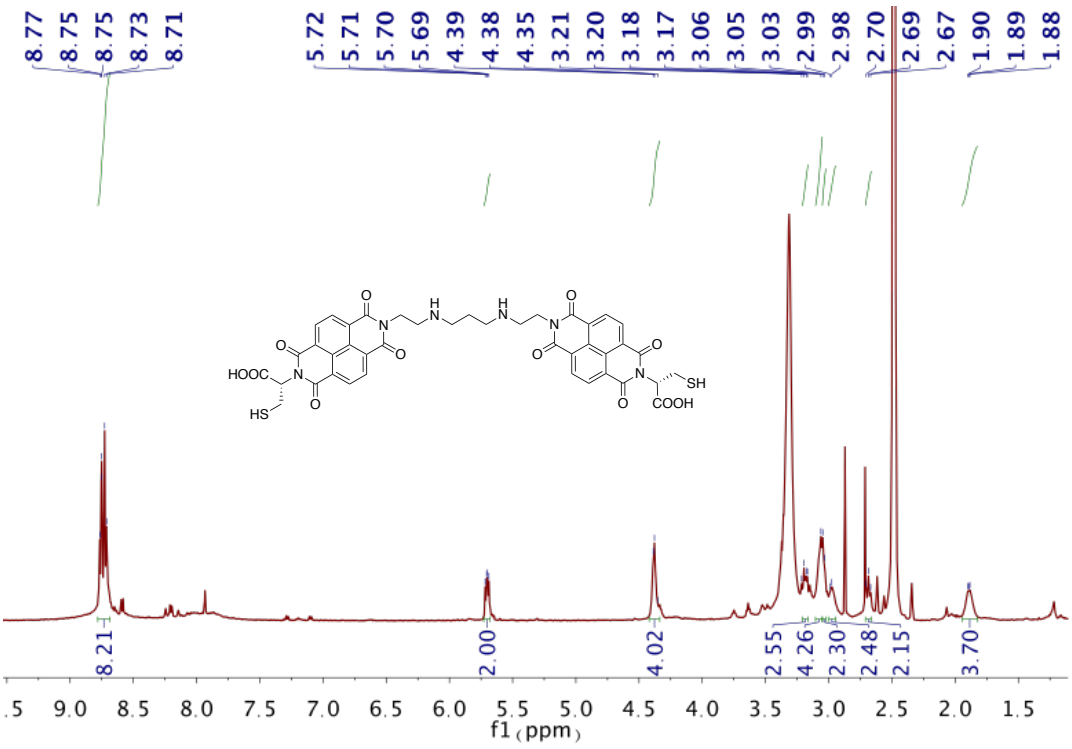

Figure S61. ^{1}H NMR of **A2*** deprotected. The peaks that have not been integrated correspond to solvent impurities such as water and DMF.

17. High Resolution Mass Spectrometry

A1 Protected

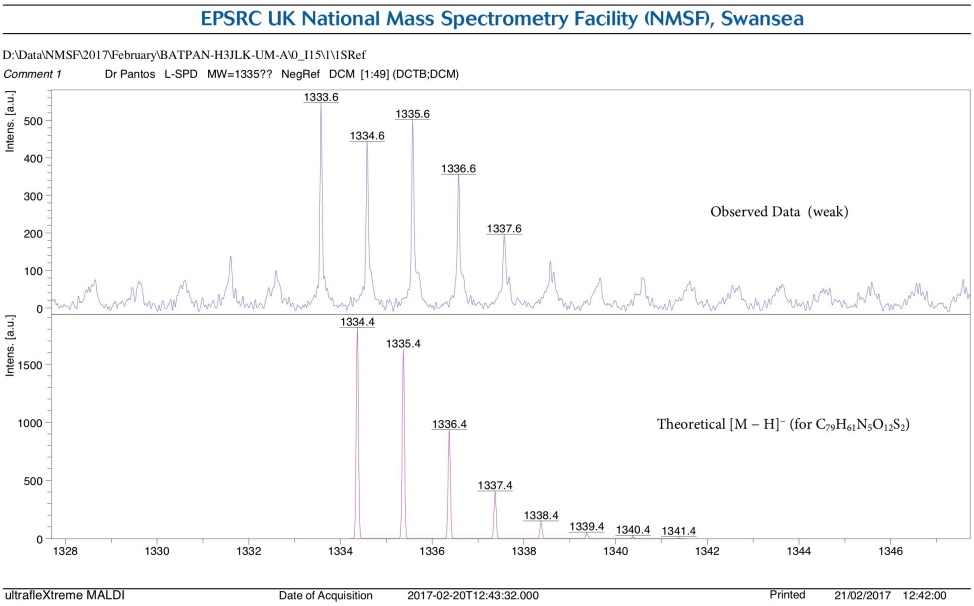

Figure S62. HRMS of **A1** protected building block.

A1* Protected

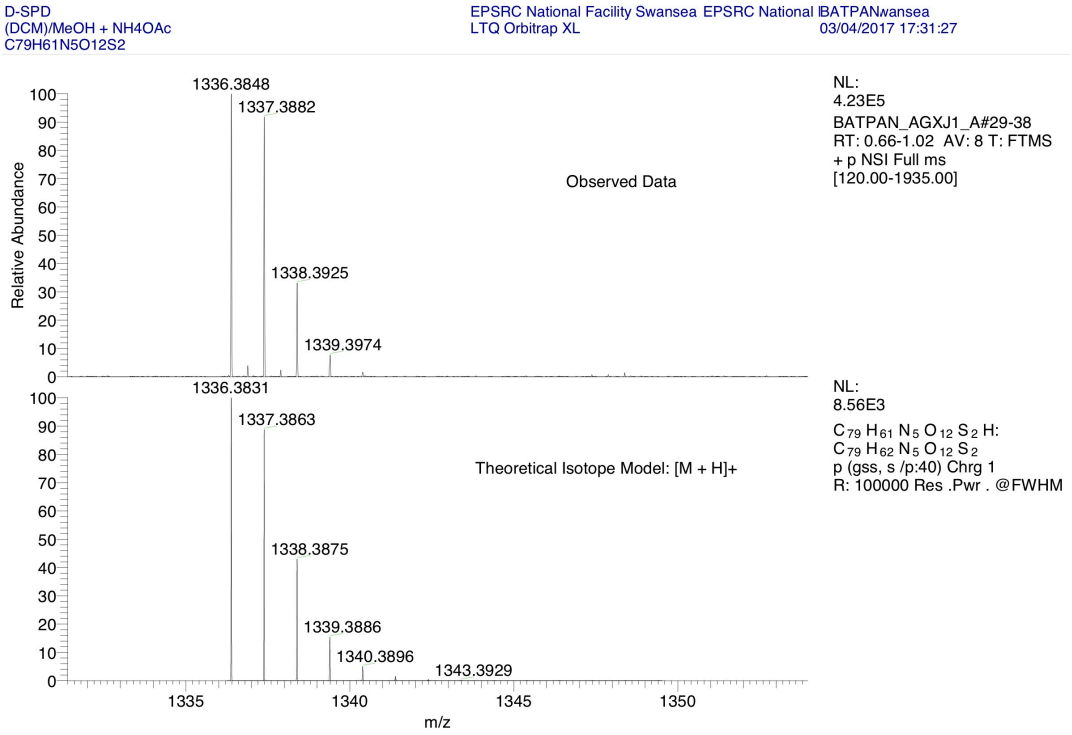

Figure S63. HRMS of **A1*** protected building block.

A2 Protected

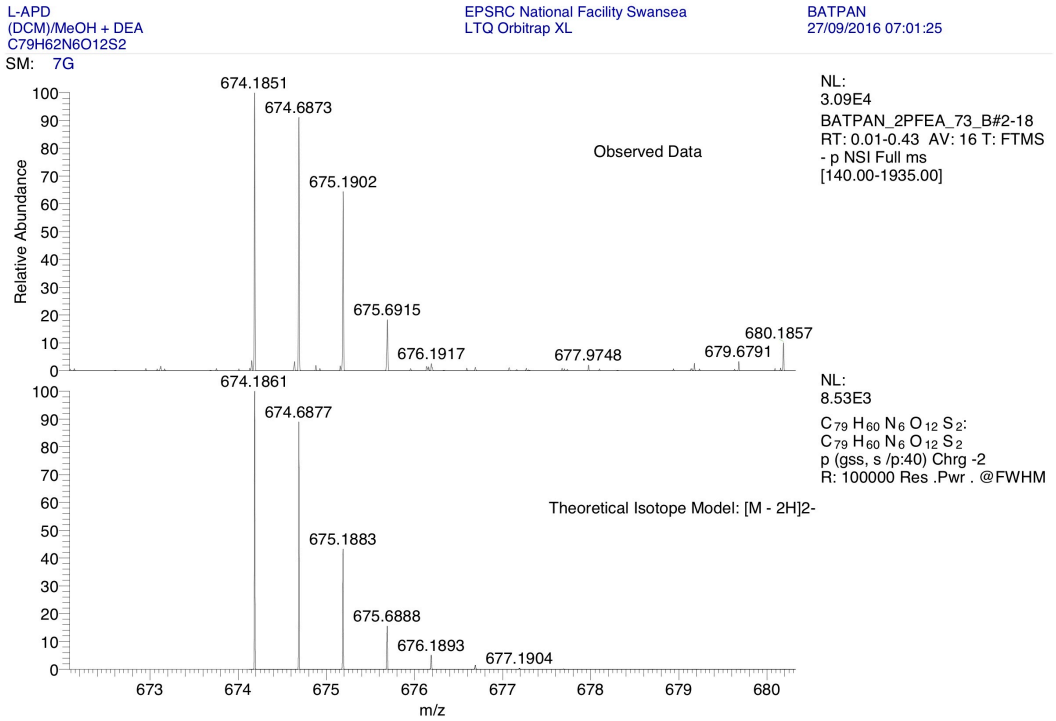

Figure S64. HRMS of **A2** protected building block.

A2* Protected

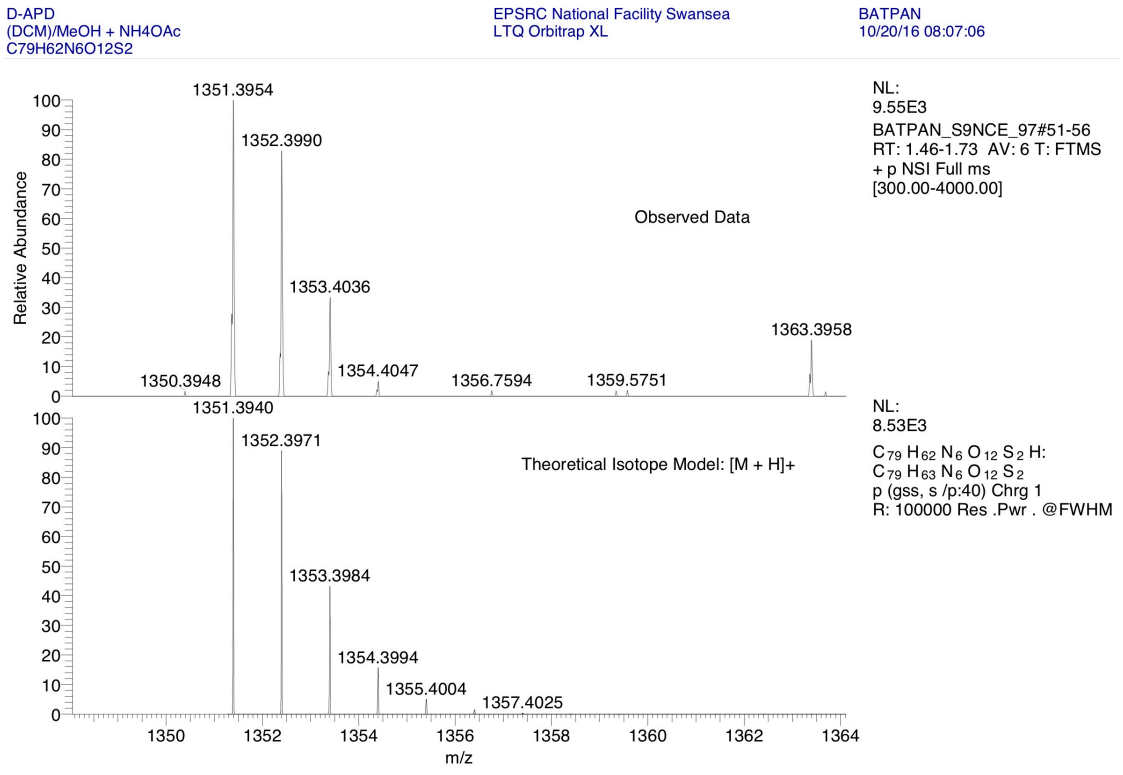

Figure S65. HRMS of **A2*** protected building block.